Radiative transfer in multifractal clouds

R. Borde, Harumi Isaka

JOURNAL OF GEOPHYSICAL RESEARCH, VOL. 101, NO. D23, PAGES 29,461–29,478, DECEMBER 27, 1996

Radiative transfer in multifractal clouds

Régis Borde and Harumi Isaka

Laboratoire de Météorologie Physique, Université Blaise Pascal, Aubière, France

Abstract. We studied effects of the cloud inhomogeneity in subcloud scale on the reflectance, transmittance, and absorptance of two-dimensional, inhomogeneous clouds. We generated the inhomogeneous clouds as multifractal clouds with a lognormal multiplicative process. For such clouds, the information codimension C_1 is a measure of the cloud inhomogeneity. Radiative transfer through the multifractal clouds was computed with a discrete angle radiative transfer model. The average reflectance, transmittance, and absorptance of multifractal clouds with a given codimension were estimated as averages of 200 realizations. They were computed for different sets of the C_1 parameter, cloud total optical thickness, and asymmetry factor of cloud scatterers. An effective optical thickness of inhomogeneous clouds was defined empirically in the framework of a homogeneous, plane parallel cloud model. Consequently, computation of radiative flux in an inhomogeneous cloud could be transformed into that of an equivalent homogeneous, plane parallel cloud. For a two-dimensional, inhomogeneous, absorbing cloud we found that an inhomogeneous cloud absorbs generally less energy than its homogeneous counterpart. An exception was found for inhomogeneous clouds characterized by a small information codimension, a large cloud optical thickness, and a large single-scattering albedo and for which absorptance is much larger than for their homogeneous counterpart. However, this increase was less than 5% of the homogeneous cloud absorptance. The use of the effective optical thickness also enabled us to treat an inhomogeneous absorbing cloud as an equivalent homogeneous absorbing cloud and to estimate the radiative flux of the equivalent homogeneous cloud as an approximation to the one in the inhomogeneous cloud. We found no immediate need to conceive of a direct effect of the cloud inhomogeneity on the single-scattering albedo, as far as we considered this treatment as a first-order approximation. We discussed the use of the effective optical thickness in two-stream radiative approximations. We also compared our results with those based on the independent pixel approximation.

1. Introduction

The effect of clouds on the radiation budget of the atmosphere is one of the fundamental issues for the study and modeling of the climate. Radiative fluxes and absorption in the clouds are frequently estimated in the framework of a uniform plane-parallel cloud and two-stream approximation [*Coakley and Chylek*, 1975; *Joseph et al.*, 1976; *Stephens*, 1978a, b; *Meador and Weaver*, 1980; *Zdunkowski et al.*, 1980]. Recent studies tend to show that the absorption of solar energy by clouds might be much larger than that expected from typical cloud radiative transfer models and call into question the real effect of clouds on the atmosphere and Earth radiation budgets [*Ramanathan et al.*, 1995; *Cess et al.*, 1995].

The area-averaged albedo and transmission of broken cloud fields have been investigated by many physicists [*Aida*, 1977; *Wendling*, 1977; *Schmetz*, 1984; *Welch and Wielicky*, 1984; *Joseph and Kagan*, 1988; *Bréon*, 1992; *Barker*, 1992]. In these studies the broken cloud fields were generated by distributing randomly or regularly clouds with simple geometrical shapes and different sizes over a limited area. The clouds were also assumed to have uniform microphysical characteristics. The cloud shapes and distributions assumed in these studies were quite idealized, when compared with those in real broken cloud fields. The radiative transfer through the broken cloud fields still remains one of the major issues in the theory of atmospheric radiation.

Clouds, even apparently homogeneous stratiform clouds, exhibit a highly inhomogeneous distribution of liquid or ice water content at subcloud scale induced by turbulent air motion [*Duroure and Guillemet*, 1990; *Brenguier*, 1990]. The inverse convection induced by radiative cooling at the cloud top also plays an important role in generating inhomogeneity in extended stratiform clouds. Such inhomogeneity in the microphysical properties may have significant influence on the radiative properties of the clouds. Effects of such cloud inhomogeneity have been discussed in relation to the unexplained cloud absorption-albedo anomaly [*Davis et al.*, 1990; *Stephens and Tsay*, 1990]. Effects of the cloud inhomogeneity were studied for various kinds of fluctuations of the optical thickness: sinusoidal variations [*Weinman and Swarztrauber*, 1968], stochastic variations [*Mikhaylov*, 1982], or experimentally observed variations of liquid water content [*Welch and Wielicki*, 1984; *Cahalan et al.*, 1994a, b]. However, there still is no well-established theoretical framework to deal with the radiative transfer in inhomogeneous media [*Fouquart et al.*, 1990].

The classical approach of this problem was often limited to study relationships between microphysical and optical properties of the inhomogeneous clouds at a "characteristic" scale, though the interaction between clouds and radiation occurs

Paper number 96JD02200.
0148-0227/96/96JD-02200$09.00

over a wide range of scales [*Lovejoy and Schertzer*, 1992]. *Lovejoy et al.* [1990], *Gabriel et al.* [1990], and *Davis et al.* [1990] studied recently the radiative transfer in fractal clouds with conservative scatterers, by using a discrete angle radiative transfer (DART) model with a four- or six-stream scattering phase function. They showed that the albedo and transmission through fractal clouds could be expressed as a function of the total cloud optical thickness and cloud fractal dimension. *Barker* [1992] and *Evans and Stephens* [1993] also discussed the radiative transfer in inhomogeneous clouds. *Barker* [1992] suggested a possible adaptation of homogeneous, plane parallel radiative transfer model to capture effects of the cloud inhomogeneities. More recently, *Cahalan et al.* [1994a, b] proposed an effective optical thickness of inhomogeneous cloud based on the independent pixel approximation (IPA).

The purpose of the present study is also to examine the possibility to transform the radiative transfer in the inhomogeneous clouds into the usual framework of uniform plane parallel clouds. Such a transformation, if possible, should be of practical importance for the radiative flux computation in climate modeling as well as for the retrieval of cloud parameters from spaceborne radiometer data. We simulated radiative transfer by using the DART model in horizontally and vertically multifractal clouds generated with a lognormal multiplicative process [*Monin and Yaglom*, 1975a, b] in vertical plane.

Fluctuations of the water content in a multifractal cloud generated by a pure multiplicative process are more intermittent than those in natural clouds. In spite of this unnaturalness, we adopted the lognormal multiplicative process because the cloud inhomogeneity can be completely characterized by the information codimension C_1. No such parameter has been defined yet to describe completely the intermittency of natural clouds. This uniqueness of the inhomogeneity parameter should make it easier to analyze simulations and parameterize the intermittency effect on the cloud radiative properties. Since the present study mainly aims to show a feasibility of such approach, the precise representation of the cloud inhomogeneity may be expected not to be essential to its results.

We have defined an effective optical thickness of an inhomogeneous cloud and shown how this parameter varies with cloud characteristics: the C_1 parameter, total optical thickness of the cloud, and asymmetry factor of the scattering phase function. The study was extended to the case of nonconservative scatterers to investigate effects of cloud inhomogeneity on the radiative properties of absorbing clouds. We evaluated how the absorptance of inhomogeneous clouds varies as a function of the information codimension C_1, total optical thickness τ_0, and single scattering albedo ω_0. Then, we examined how the effective optical thickness could be integrated into the framework of the plane parallel homogeneous cloud and that of typical two-stream approximations. Finally, we compared our evaluation of effective optical thickness with those derived from the IPA.

2. Generation of Multifractal Clouds

To investigate effects of the cloud inhomogeneity on the cloud radiative properties, we need not only to generate an inhomogeneous cloud, but also to estimate statistical parameters that provide a complete quantitative description of the cloud inhomogeneity. This is not an easy task because we still do not know what is meant by a complete quantitative description of the cloud inhomogeneity or what aspect of the inhomogeneity has effective influence on the cloud radiative properties.

Many physicists have recently had recourse to the fractal and multifractal analysis of real clouds and cloud fields to investigate their scaling and autosimilarity properties [*Lovejoy*, 1982; *Duroure and Guillemet*, 1990; *Joseph and Cahalan*, 1990; *Marshak et al.*, 1994; *Tessier et al.*, 1993]. The grounds for this recourse are that the degree of inhomogeneities can be characterized with only a few parameters, but these parameters, once estimated, can be used to generate other fields with the same multifractal characteristics [*Schertzer and Lovejoy*, 1991; *Davis et al.*, 1993; *Marshak et al.*, 1994].

A multifractal medium can be easily generated with multiplicative cascade process [*Monin and Yaglom*, 1975a, b; *Parisi and Frisch*, 1985]; this process is also called "weighted curdling" by *Mandelbrot* [1983]. The lognormal process used here follows that formalized by Yaglom as a model of eddy breakdown and described by *Monin and Yaglom* [1975a, b]. One starts with an initial homogeneous field (in our case a homogeneous square) with a given total mass M_0 of scatterers. One subdivides this initial square into four subsquares, and afterwards, repeats the same operation to each newly formed subsquare. After n steps of subdividing, the initial square is divided into 2^{2n} subsquares. At each step of subdividing, the mass in a subsquare is distributed over four newly created subsquares according to a prefixed rule of cascade. Mass in a cell after n steps is given by

$$m_n = m_{n-1}\alpha_n = M_0\alpha_1\alpha_2 \cdots \alpha_n, \tag{1}$$

where M_0, m_{n-1} and m_n are the mass in the initial square, $n-1$th and nth step cells, respectively; α_j is a multiplicative factor at the jth subdividing step. Different rules can be defined and adopted to select the multiplicative factor α at each subdividing step. The mass distribution at large scale modulates multiplicatively the mass at smaller scale, which assures the self-similarity and scale invariance of the field and creates a hierarchy of singularities. Stochastic variables $\ln \alpha_1, \cdots, \ln \alpha_n$ are assumed to have a normal distributions with a mean η and a variance μ^2. Hence the mean and the variance of the variable $\ln m_n$ can be expressed as

$$\begin{aligned} \bar{m}_n &= \overline{\ln (m_n)} = \ln (M_0) + A(\mathbf{x}) + n\eta \\ \sigma_n^2 &= A_1(\mathbf{x}) + n\mu^2 \end{aligned} \tag{2}$$

where $A(\mathbf{x})$ and $A_1(\mathbf{x})$ represent the effect of the first few coefficients α_i.

In this way, an initial homogeneous distribution of the mass M_0 is transformed into an inhomogeneous distribution over the same area. The mean of the variable m_n is independent of the observation scale λ_n $(= L_0/2^n)$, where L_0 is the size of the initial square. Consequently, the mean η is related to the variance μ^2 of the Gaussian generator by $\eta = -\mu^2/2$ [*Monin and Yaglom*, 1975a]. The qth order statistical moment of m_n may be written as

$$\overline{m_n^q} = M_0^q \exp\{\tfrac{1}{2}q(q-1)(\sigma_n^2 + A_1)\} \approx M_0^q(\lambda_n/L_0)^{-1/2q(q-1)\mu^2} \tag{3}$$

This expression is formally identical with the qth-order statistical moment of a multifractal field $\varepsilon_\lambda(\mathbf{x})$ at an observation scale λ [*Schertzer and Lovejoy*, 1987]:

$$\overline{\varepsilon_\lambda(\mathbf{x})^q} \propto \lambda^{-K(q)} \tag{4}$$

where the function $K(q)$ is a convex function with predetermined values $K(0) = K(1) = 0$. A generalized dimension D_q is defined by

$$D_q = D - \frac{K(q)}{q - 1} \tag{5}$$

and the information codimension C_1 is defined by

$$C_1 = D - D_1 = \left\{\frac{dK(q)}{dq}\right\}_{q=1} \tag{6}$$

where D is the topological dimension of the space [*Hentschel and Procaccia*, 1983]. The information codimension C_1 represents a measure of intermittency of the field. As C_1 increases from 0 for a homogeneous medium to D, the total mass of the scatterer tends to be distributed over fewer and fewer points; for $C_1 = D$, all the mass is found at a randomly positioned single point. A case with $C_1 > D$ is called "degenerated," meaning that every realization is empty and, now and then, a realization occurs with a huge peak [*Davis et al.*, 1993]. By equating the exponent of (3) with the function $K(q)$, we have

$$K(q) \approx \tfrac{1}{2}q(1 - q)\mu^2. \tag{7}$$

The multifractal field generated by a lognormal multiplicative process with $\eta = -\mu^2/2$ has an information codimension $C_1 = \mu^2/2$. In other words, a multifractal field with a given C_1 can be generated by choosing the variance of the lognormal distribution $\mu^2 = -2\eta = 2C_1$. Such a multifractal field is a nonlacunary and dense fractal according to *Mandelbrot*'s [1983] terminology.

The one-dimensional (1-D) spatial correlation of the lognormal field can be expressed in the form

$$b_{\varepsilon\varepsilon}(|\mathbf{r}|) = \overline{\varepsilon(\mathbf{x})\varepsilon(\mathbf{x} + \mathbf{r}) - \varepsilon(\mathbf{x})^2} \propto (L/r)^{\mu^2}, \tag{8}$$

where r and L are the observation and external scales, respectively [*Monin and Yaglom*, 1975a, b]. Generally, the correlation decreases with the distance r, but for too rapid decay ($\mu^2 > 1$), the correlation becomes basically a "quasi-δ correlation" [*Marshak et al.*, 1994].

The Fourier spectrum $S(\kappa)$ corresponding to this autocorrelation function is given by

$$S(\kappa) \propto \kappa^{-1+\mu^2} = \kappa^{-\beta} \tag{9}$$

where κ is the wave number. Since the variance μ^2 is positive, the spectrum slope cannot be steeper than -1 as C_1 approaches 0. Therefore fluctuation spectra generated by a pure multiplicative cascade process are flatter than those of liquid water content in real clouds, for which spectral slopes between $-3/2$ and -3 were often reported [*King et al.*, 1981; *Barker*, 1992]. *Marshak et al.* [1994] tried to remedy this limitation in spectral slope, by introducing a second multifractal parameter H_1, which represents a "nonstationary" state of fluctuations. Shortcomings of the lognormal process were also discussed by *Frisch* [1996].

In spite of this unnatural feature of pure multiplicative cascade fields, we still used two-dimensional multifractal clouds generated with lognormal multiplicative process. We did so because we have investigated the impact of cloud inhomogeneity on the radiative transfer as a function of other cloud optical parameters (total cloud optical thickness, asymmetry factor and single-scattering albedo of the scatterers) and we had to keep the number of parameters used to generate the inhomogeneous clouds as small as possible. The lognormal multiplicative process generates a "one-parameter-controlled" inhomogeneous medium, in which both the probability distribution and the spatial correlation of fluctuations are defined by the information codimension C_1. As was mentioned above, this made the search for an empirical relationship between radiative properties and inhomogeneity parameter of the clouds significantly easier.

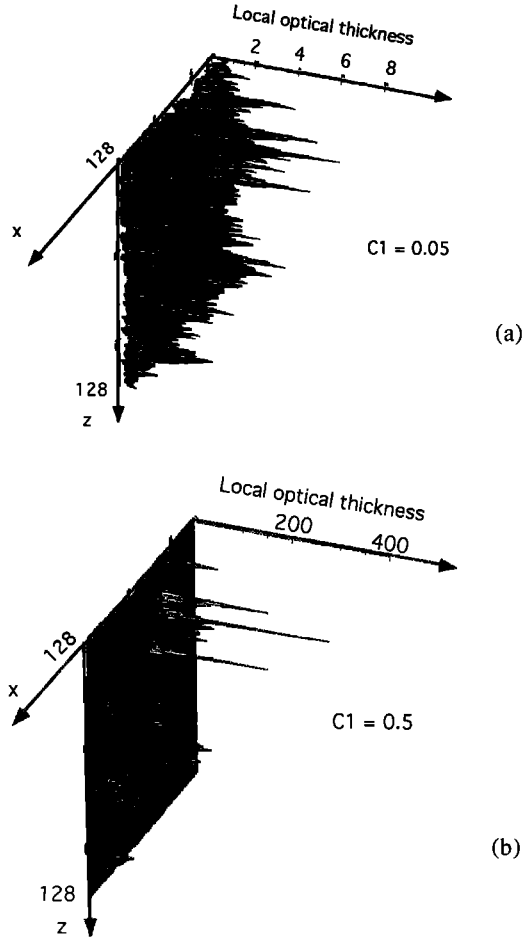

Figure 1. Multifractal fields of the scatterer mass generated with a multiplicative lognormal cascade process and different information codimensions: (a) $C_1 = 0.05$ and (b) $C_1 = 0.5$. Both fields have the same total mass of the scatterer.

Like other random cascade models, the lognormal process is nonconservative, [*Frisch*, 1996], so after we generated a multifractal cloud, we recomputed the total mass of the generated cloud by adding the mass of all the elementary cells. When this recomputed mass differed from the initial one, we corrected the mass in each elementary cell by multiplying it with a correction factor and conserved the initial mass of the cloud. To illustrate how the cloud inhomogeneity varies with C_1, we reproduced examples of two-dimensional (2-D, x-z) multifractal clouds generated with the C_1 parameter respectively of 0.05 and 0.5 (Figures 1a and 1b). As C_1 increases from 0.05 to 0.5, the mass becomes distributed over fewer cells, and the local density of these cells becomes much higher.

3. Discrete Angle Radiative Transfer Model

To compute the radiative transfer in a 2-D multifractal cloud such as those presented above, we have two options: a Monte

Carlo code or a discrete angle radiative transfer code in which light scatters only in a limited number of angular directions. The DART model with a four-stream (six streams for 3-D case) scattering phase function was previously used to compute radiative transfer in fractal media [*Lovejoy et al.*, 1990; *Gabriel et al.*, 1990; *Davis et al.*, 1990; *Gierens*, 1993]. Although the DART model implies overhead sun and a limited number of scattering directions, it nevertheless allows the effects of cloud inhomogeneity to be studied in some detail. It also requires much less computing time. Hence we adopted the DART model in this study.

By discretizing the radiative transfer equation, the DART equation can be expressed for a four-stream scattering function in the following form:

$$I(\mathbf{x}, u) = I(\mathbf{x} - u\delta\mathbf{x}, u) - I(\mathbf{x}, u)\delta\tau + \omega_0\sigma_{u,u}I(\mathbf{x}, u)\delta\tau + \sum_{v\neq u} \omega_0\sigma_{u,v}I(\mathbf{x} - v\delta\mathbf{x}, v)\delta\tau \quad (10)$$

where $I(\mathbf{x}, u)$ is the intensity in the direction of propagation u at a position $\mathbf{x}$. The quantity ω_0 represents the single-scattering albedo of the cloud scatterer, and the local optical thickness of a cell is given by $\delta\tau = \sigma\rho(\mathbf{x})\delta x$, where σ, $\rho(\mathbf{x})$, and δx are the extinction coefficient, scatterer density, and size of the elementary cell, respectively. The quantity $\sigma_{u,v}$ represents the fraction of the energy scattered from the direction v into the direction u. Equation (10) is obtained by discretizing the direct light in the implicit mode and discretizing the side scattering and reflection in the explicit mode. This semi-implicit equation differs from the explicit mode used by *Lovejoy et al.* [1990], *Gabriel et al.* [1990], and *Davis et al.* [1990]. Local transmittance and reflectance are expressed for the explicit and semi-implicit discretizations in the following forms:

Explicit mode

$$t = \frac{I(\mathbf{x} + u\delta\mathbf{x}, u)}{I(\mathbf{x}, u)} = 1 - \delta\tau(1 - \omega_0\sigma_{u,u}) \qquad r = \frac{I(\mathbf{x} - u\delta\mathbf{x}, -u)}{I(\mathbf{x}, -u)} = \delta\tau\omega_0\sigma_{u,-u} \quad (11a)$$

Semi-implicit mode

$$t = \frac{I(\mathbf{x}, u)}{I(\mathbf{x} - u\delta\mathbf{x}, u)} = \frac{1}{1 + \delta\tau(1 - \omega_0\sigma_{u,u})} \qquad r = \frac{I(\mathbf{x}, -u)}{I(\mathbf{x} + u\delta\mathbf{x}, u)} = \frac{\delta\tau\omega_0\sigma_{u,-u}}{1 + \delta\tau(1 - \omega_0\sigma_{u,u})} \quad (11b)$$

The energy side-scattered or absorbed by a cell is expressed respectively by

$$s = \frac{\delta\tau\omega_0\sigma_{u,u\perp}}{1 + \delta\tau(1 - \omega_0\sigma_{u,u})} \qquad a = \frac{\delta\tau(1 - \omega_0)}{1 + \delta\tau(1 - \omega_0\sigma_{u,u})} \quad (11c)$$

In the explicit mode, we have $t \to -\infty$ and $r \to \infty$ as $\delta\tau \to \infty$, while $t \to 0$ and $r \to \omega_0\sigma_{u,-u}/(1 - \omega_0\sigma_{u,u})$ as $\delta\tau \to \infty$. This means that in the case of a cell with a very high local optical thickness the explicit mode would not provide correct local values of transmittance and reflectance [*Gierens*, 1993]. The asymmetry factor is equal to $g = \sigma_{u,u} - \sigma_{u,-u}$. For the conservative scattering, we verify $\sigma_{uu} + 2\sigma_{u,u\perp} + \sigma_{u,-u} = 1$ and $r + 2s \to 1$ as $\delta\tau \to \infty$ in the semi-implicit mode. *Davis et al.* [1990] showed that the transmitted and reflected energy computed by means of a DART model agreed with those obtained with a Monte Carlo code and validated the DART approach in computing radiative fluxes in inhomogeneous clouds.

The cloud top was illuminated with a uniform normalized flux of incident energy. Equation (10) was solved numerically by a relaxation method. Iterations were stopped when the difference between sums of incoming ($I_+(0) = 1$ and $I_-(\tau_0) = 0$) and outgoing ($I_-(0)$ and $I_+(\tau_0)$) fluxes was less than 0.1% for a conservative scattering and when the transmitted, reflected, and absorbed energies at every pixel in the domain did not change more than 0.1% during an iteration for absorbing clouds. Clouds were simulated in a domain of 128 × 128 square cells, each cell having a local value of cloud optical thickness $\delta\tau_{ij}$. We adopted a cyclic lateral condition. The semi-implicit scheme can also provide exact two-stream solutions for a homogeneous cloud with the conservative scattering and cyclic lateral boundary conditions.

4. Definitions of the Average Transmittance, Reflectance and Optical Thickness in Inhomogeneous Clouds

Figures 2a and 2b illustrate the simulated transmission of light in a homogeneous cloud and an inhomogeneous cloud, respectively. The transmission of light through the inhomogeneous cloud varies from point to point as a function of the spatial distribution of scatterers, while the transmission in the homogeneous cloud changes regularly with the distance from the cloud top. Light penetrates deeply into the less dense part of the cloud and hardly through much denser parts. Evaluating the influence of cloud inhomogeneity corresponds to evaluating the nonlinear contribution of this larger transmission of light through optically thinner parts in the cloud.

The optical thickness in a homogeneous cloud varies proportionally as a function of the geometrical depth, while such a proportionality cannot be valid for an inhomogeneous cloud. Therefore in dealing with an inhomogeneous cloud, we need to define an average optical thickness in a way compatible with both homogeneous and inhomogeneous clouds. We defined the average optical thickness at the ith level as the vertical sum from the first to the ith layer of the horizontally averaged local optical thickness:

$$\tau_i = \sum_{j=1}^{i} \langle \delta\tau_{lj} \rangle_j, \quad (12a)$$

where $\langle\ \rangle_j$ designates the average over n cells ($\delta\tau_{lj}$, $l = 1, \cdots, n$) in the jth layer. According to this definition, the total average optical thickness of the inhomogeneous cloud can be kept identical with that of the homogeneous cloud. The average optical thickness in the inhomogeneous cloud does not vary linearly with the geometrical depth as in the homogeneous cloud. The total transmittance T_i at the ith layer is the horizontal sum of transmitted energy T_{li} through n cells in the ith layer:

$$T_i = \sum_{l=1}^{n} T_{li}. \quad (12b)$$

The horizontal average and sum are taken over the largest horizontal scale of fluctuations of scatterers concentration in the cloud. This scale is equal to the side length L_0 of the cloud domain in the present study.

When one generates inhomogeneous clouds with a given mass of scatterers and a given C_1, there are an infinite number of inhomogeneous clouds that are apparently different. This also arises a need to estimate the average radiative behavior of inhomogeneous clouds as an set average over all the possible realizations. A two-dimensional distribution of frequency of occurrence was estimated as a function of transmittance and optical thickness for a set of 200 clouds (Figure 3). Each cloud has the same set of parameters: a total optical thickness of $\tau_0 = 20$, an asymmetry factor $g = 0$, a geometrical depth of $128\Delta z$ (where Δz is the thickness of each layer), and $C_1 = 0.2$.

We reproduced histograms of the transmittance for four different values of the average optical thickness, $\tau = 4$, 8, 12, and 16 (Figure 4). The mean and standard deviation are

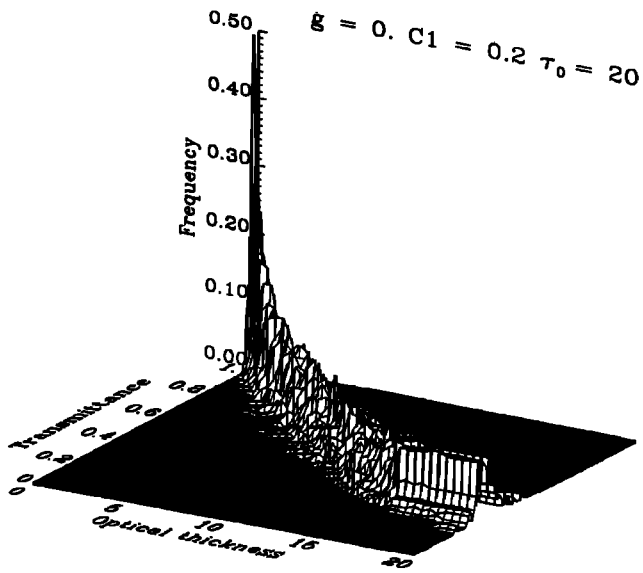

Figure 3. Joint distribution of frequency of occurrence as a function of the transmittance and optical thickness. The frequency of occurrence was estimated from 199 realizations of the inhomogeneous cloud with a total optical thickness of 20 and an information codimension of 0.2.

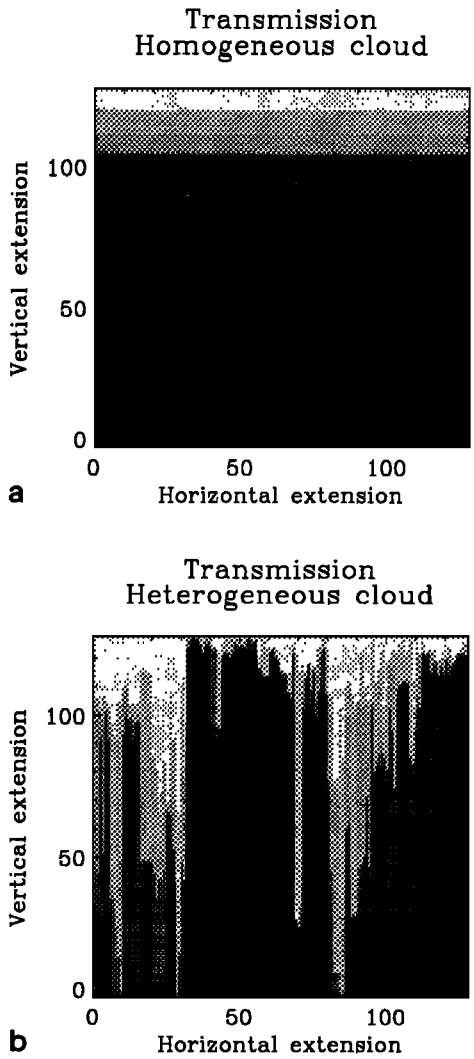

Figure 2. Intensity of transmitted light through (a) a homogeneous cloud and (b) an inhomogeneous cloud as computed with the DART model. Both the clouds have same average total optical thickness of 20. The inhomogeneous cloud is generated with an information codimension of 0.3.

0.822 ± 0.042, 0.664 ± 0.060, 0.501 ± 0.063, and 0.335 ± 0.047, respectively. The skewness is slightly negative for $\tau = 4$ and positive for other values of τ, and the tail of the distribution becomes more important for large τ. We tested the Gaussianity of these distributions by applying χ^2 and Kolmogorov-Smirnov tests to the cumulative frequency of occurrence. The tests showed that all the distributions could be considered as normal distribution at a significant level of 10%.

We computed the transmittance in other inhomogeneous clouds with the same mass of scatterers ($\tau_0 = 20$), but with different C_1 parameters. The standard deviation increases with C_1 (Table 1), because the mass distribution of a multifractal cloud with a large C_1 has fewer and more intermittent singularities and consequently changes considerably from one realization to another.

5. Radiative Fluxes Through Multifractal Clouds in Conservative Scattering

5.1. Variation of the Transmittance With C_1

In Figure 5 we plotted the average transmittance as a function of the average optical thickness for inhomogeneous clouds with the same total optical thickness $\tau_0 = 20$ and different values of C_1. The line labeled "homog" presents the transmittance with the optical depth in the homogeneous cloud, which is a linear function with a slope of $-1/(2 + \tau_0)$. For $\tau < 3$ the transmittance through the inhomogeneous clouds decreases with the optical thickness in the same way for all C_1. In the range $\tau > 3$ the transmittance through inhomogeneous clouds decreases almost linearly as a function of the average optical thickness for any value of C_1. As the optical thickness becomes large, more photons can interact with the scatterers, and the multiple scattering becomes more important. Hence the transmission of light is more dependent on the spatial inhomogeneity of the scatterers.

The transmittance for a given optical thickness increases

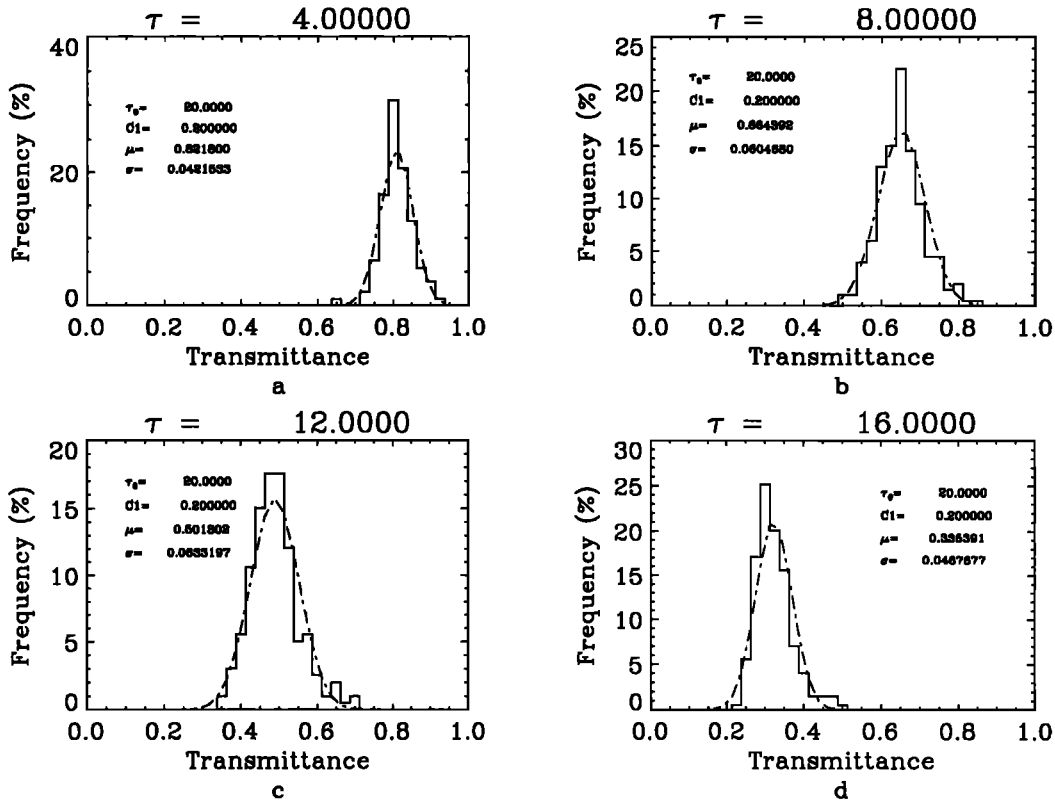

Figure 4. Histograms of the transmittance at four different average optical thickness (τ = 2, 4, 8, and 16). The histograms are established from 199 realizations of the inhomogeneous cloud with a total optical thickness of 20 and an information codimension of 0.2. The estimated means and standard deviations of these histograms are 0.822 ± 0.042, 0.664 ± 0.060, 0.501 ± 0.063, and 0.335 ± 0.047 for τ = 2, 4, 8, and 16, respectively; the normal distributions with these means and standard deviations are plotted.

with C_1 because more light is transmitted through the part of the cloud with smaller local optical thickness. Figure 5 confirms that an inhomogeneous cloud transmits a greater amount of energy than a homogeneous one. Since the scattering is supposed to be conservative, an inhomogeneous cloud has a smaller albedo than a homogeneous one.

5.2. Definition of an Effective Optical Thickness

These inhomogeneity effects may be taken into account by defining an "effective optical parameter" as a function of C_1. A basic idea is to define this effective optical parameter so that the radiative transfer in inhomogeneous clouds might be treated in the classical framework of a plane parallel homogeneous cloud. Such a definition should take into account not only the C_1 parameter but also the asymmetry factor g of the

Table 1. Variation of the Standard Deviation of the Transmittance at Four Optical Thickness in Inhomogeneous Clouds

	Standard Deviation of Transmittance			
C_1	τ = 4	τ = 8	τ = 12	τ = 16
0.1	0.022	0.033	0.033	0.023
0.2	0.042	0.060	0.063	0.047
0.3	0.049	0.073	0.076	0.060
0.4	0.059	0.081	0.089	0.079
0.5	0.066	0.097	0.109	0.100
0.6	0.063	0.089	0.102	0.098

The inhomogeneous clouds are generated for a given total optical thickness of 20 with different information codimensions C_1. The standard deviation are estimated as an ensemble average over 199 realizations.

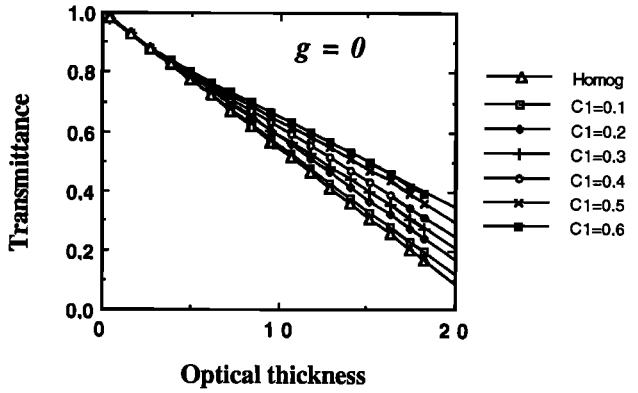

Figure 5. Variation of the transmittance in inhomogeneous clouds as a function of the average optical thickness. The transmittance is computed as an ensemble average over 200 realizations of the inhomogeneous cloud with the same cloud characteristics. The inhomogeneous clouds have the same total optical thickness of 20, but they are generated for different information codimensions (C_1 = 0, 0.1, 0.2, 0.3, 0.4, 0.5, and 0.6); the cloud with C_1 = 0 represents a homogeneous cloud.

scatterers and the cloud total optical thickness τ_0. For simplicity, we will first define this effective optical thickness as a function of only C_1 and afterward consider the effects of the other parameters.

An effective optical thickness τ' of an inhomogeneous cloud is defined as the optical thickness of an "equivalent" homogeneous cloud that would have the same transmittance as that of the inhomogeneous cloud. This is shown schematically in Figure 6. $T(\tau, \tau_0, C_1)$ represents the transmittance for an optical thickness of τ, through a cloud with a total optical thickness τ_0, and C_1. For conservative scattering, the global transmittance of a homogeneous cloud with a total optical thickness τ_0 is given by the two-stream approximation solution: $T(\tau_0, \tau_0, C_1 = 0) = 2/[2 + (1 - g)\tau_0]$ [*Meador and Weaver*, 1980]. The curve labeled "2 streams" represents this relation.

An equivalent homogeneous cloud is a homogeneous cloud that has the same total transmittance as that of the inhomogeneous cloud. The total optical thickness τ_0' of the equivalent homogeneous cloud is given by the relation

$$T(\tau_0', \tau_0', C_1 = 0) = \frac{2}{2 + (1 - g)\tau_0'} = T(\tau_0, \tau_0, C_1 = 0.5) \tag{13}$$

where $T(\tau_0', \tau_0', C_1 = 0)$ and $T(\tau_0, \tau_0, C_1 = 0.5)$ designate the global transmittance of the equivalent homogeneous cloud with a total optical thickness of τ_0' and that of the inhomogeneous cloud with a total optical thickness of τ_0 and a C_1 of 0.5, respectively. The total optical thickness of the equivalent homogeneous cloud is the "effective" total optical thickness of the inhomogeneous cloud. The straight line labeled "equiv homog" represents the transmittance in a homogeneous cloud that is equivalent to the inhomogeneous cloud labeled "$C_1 = 0.5$". The slope of the "equiv.homog" line is given by $2/[2 + (1 - g)\tau_0']$. The "effective" optical thickness of the "$C_1 = 0.5$" inhomogeneous cloud is estimated by taking the correspondence:

$$T(\tau', \tau_0', C_1 = 0) = T(\tau, \tau_0, C_1 = 0.5). \tag{14}$$

This equation means the transmittance $T(\tau', \tau_0', C_1 = 0)$ for an optical thickness τ' in an equivalent homogeneous cloud ($C_1 = 0$) is identical with that $T(\tau, \tau_0, C_1 = 0.5)$ for an optical thickness τ in an inhomogeneous cloud ($C_1 = 0.5$).

We applied this transformation of the average optical thickness τ into the equivalent optical thickness τ' to all the curves in Figure 5. The effective optical thickness τ' is plotted as a function of the average optical thickness τ for various C_1 (Figure 7); the total optical thickness of the clouds is kept constant $\tau_0 = 20$. For large optical thickness ($\tau > 3$), τ' exhibits a linear variation as a function of τ. A priori, these curves should be subject to the following conditions:

$$\lim_{\tau \to 0} \tau' = 0 \tag{15a}$$

$$\lim_{C_1 \to 0} \tau' = \tau \tag{15b}$$

$$\lim_{\tau \to 0} \left(\frac{d\tau'}{d\tau} \right) = \frac{2 + (1 - g)\tau_0'}{2 + (1 - g)\tau_0} \tag{15c}$$

$$(d\tau'/d\tau)_{0 \ll \tau \leq \tau_0} = \Gamma(C_1) \tag{15d}$$

where τ, τ', and C_1 are the usual optical thickness expressed by equation (12a) the effective optical thickness, and the information codimension of the inhomogeneous cloud, respectively. The first condition is a trivial condition expressing that when the usual optical thickness is small, the corresponding equivalent optical thickness is also small. The second condition is that a homogeneous cloud is its own equivalent homogeneous cloud. The third condition results directly from the ratio between the slope of $T(\tau', \tau_0', C_1 = 0)$ and that of $T(\tau, \tau_0, C_1 = 0)$. We have already shown above that in the uppermost layer of an inhomogeneous cloud ($\tau < 3$) the inhomogeneity has little influence on the transmission: $T(\tau < 3, \tau_0, C_1 = 0)$

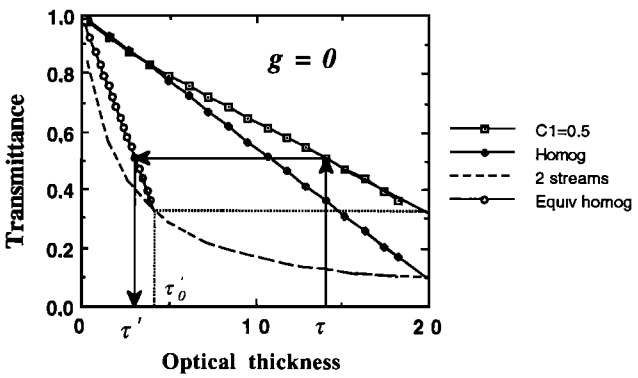

Figure 6. Schematic representation of the definition of an effective optical thickness τ' of an inhomogeneous cloud. The "$C_1 = 0.5$" curve represents the transmittance versus optical thickness relation for an inhomogeneous cloud with a total optical thickness of 20 and an information codimension of 0.5. The "homog" line represents the transmittance versus optical thickness relation for a homogeneous cloud with the same optical thickness of 20. The "equiv.homog" line represents the transmittance versus optical thickness relation of an "equivalent" homogeneous cloud that has the same global transmittance as the inhomogeneous cloud. The effective optical thickness of the inhomogeneous cloud is defined by taking the optical thickness on this line corresponding to the transmittance of the inhomogeneous cloud. The "2 streams" curve represents the global transmittance versus total optical thickness relation of a homogeneous cloud obtained under the two-stream approximation.

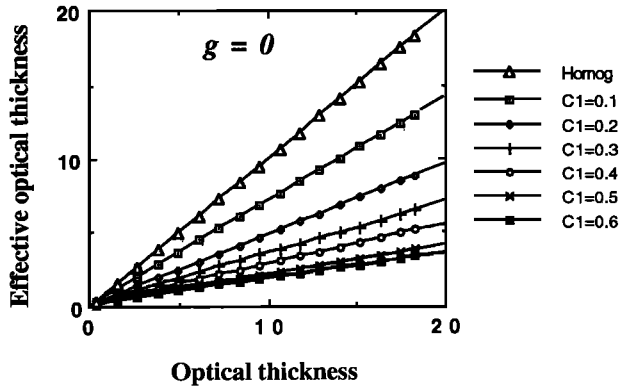

Figure 7. Variation of the effective optical thickness as a function of the optical thickness for the same inhomogeneous clouds as in Figure 5. The inhomogeneous clouds have the same total optical thickness of 20, but they are generated for different information codimensions ($C_1 = 0$, 0.1, 0.2, 0.3, 0.4, 0.5, and 0.6); the cloud with $C_1 = 0$ represents a homogeneous cloud.

$\approx T(\tau < 3, \tau_0, C_1 \neq 0)$. In spite of this fact, the corresponding effective optical thickness should depend on the degree of cloud inhomogeneity because the effective optical thickness is defined in the framework of the two-stream approximation and the total cloud optical thickness has to be transformed in the equivalent total cloud optical thickness. The fourth condition implies that for large optical thickness the effective optical thickness varies linearly with the average optical thickness of the inhomogeneous clouds and that the slope is function of the degree of inhomogeneity C_1. Accordingly, we assumed that the semiempirical expression of the equivalent optical thickness τ' can be written in the following form:

$$\tau' = \{B(C_1, \tau_0)C_1 + \Gamma(C_1)\tau\}\left\{1 - \exp\left(-\frac{\tau}{AC_1}\right)\right\}, \quad (16)$$

where A is a constant, $B(C_1, \tau_0)$ is a function of C_1 and τ_0, and $\Gamma(C_1)$ is a function of C_1 only. From (15c), we can derive the relation between A and $B(C_1, \tau_0)$:

$$B(C_1, \tau_0) = \frac{2 + (1 - g)\tau_0'}{2 + (1 - g)\tau_0}A. \quad (17)$$

By using this relation in (16) and setting $\tau' = \tau_0'$ and $\tau = \tau_0$, we obtain the expression

$$\tau_0' \approx \Gamma(C_1)(\tau_0 + C_1), \quad (18)$$

and consequently

$$B(C_1, \tau_0) = \left\{\Gamma(C_1) + \frac{2 - (2 - C_1)\Gamma(C_1)}{2 + (1 - g)\tau_0}\right\}A. \quad (19)$$

To obtain 19, we assumed that τ_0 is large enough that the exponential term can be neglected. The slope for large average optical thickness $(d\tau'/d\tau)_{\tau \gg 1} \approx \Gamma(C_1)$ varies as a function of C_1. It has to satisfy the relation $\Gamma(C_1 = 0) = 1$. Therefore it may be approximated in an exponential form:

$$\Gamma(C_1) = e^{-kC_1}. \quad (20)$$

For isotropic scattering ($g = 0$) and inhomogeneous clouds with various C_1 and $\tau_0 = 20$, we estimated the constants A and k with a nonlinear least squares method and obtained $A \approx 0.4$ and $k \approx 3.21$.

6. Variation of the Effective Optical Thickness With the Asymmetry Factor and the Total Optical Thickness of Clouds

The volume-scattering phase function of a cloud varies with microphysical characteristics (phase, size distribution, etc.) of the cloud. Compared with the isotropic scattering we used above, they have generally much larger forward scattering with an asymmetry factor around 0.85. Therefore we have to examine the dependency of the effective optical thickness τ' on the asymmetry factor g.

6.1. Contributions of the Asymmetry Factor

The effective optical thickness is computed as a function of the optical thickness τ for various values of the asymmetry factor and C_1 parameter. As for the isotropic scattering (Figure 7), the effective optical thickness τ' is found to vary almost linearly with the average optical thickness τ when it is large enough. Slopes of this linear function $(d\tau'/d\tau)_{\tau \gg 1}$ are examined as a function of C_1 for different values of g. It was found that the slope $(d\tau'/d\tau)_{\tau \gg 1}$ might be expressed with an exponential function of C_1 (equation (21)) and that (15b) and (15c) have to be satisfied for any g. These considerations lead us to assume an expression:

$$\left(\frac{d\tau'}{d\tau}\right)_{\tau \gg 1} = \Gamma(C_1, g) = \exp\left[-\gamma(g, C_1)C_1\right], \quad (21)$$

where $\gamma(g)$ is a function of the asymmetry factor g. The function $\Gamma(C_1, g)$ was assumed to be a polynomial of the second order with respect to C_1 and its coefficients as a function of the variable $(1 - g)$. A second-order polynomial is preferred here. After some trials, the following form was fitted to the computed slopes:

$$\ln \Gamma(C_1, g) = -\left\{\frac{1 - g}{0.055 + 0.195(1 - g)}C_1 + \left[0.9 - \frac{1 - g}{0.070 + 0.330(1 - g)}\right]C_1^2\right\}. \quad (22)$$

For a given g the slope $(d\tau'/d\tau)_{\tau \gg 1}$ becomes smaller and removed from 1 as C_1 increases. For a given C_1 this slope varies first moderately with g when g is less than about 0.8 and increases rapidly up to 1 as g approaches 1. For example, for $C_1 = 0.3$, the slope $(d\tau'/d\tau)_{\tau \gg 1}$ varies from 0.32 to 0.42 as g changes from 0 to 0.7 and goes up to 0.86 for $g = 0.98$. This suggests that the impact of the inhomogeneity on the radiative properties of the clouds decreases continuously as g is near 1; in the particular case of $g = 1$ the cloud inhomogeneity does not affect the transmittance of light through the cloud. This is a consequence of increased forward scattering. Energy scattered forward has the same effect as directly transmitted energy. As g increases, photons appear to have less interaction with the cloud scatterers. It is quite evident that as photons interact little with the cloud scatterers, their spatial distribution has little influence on the transmittance of the energy through the clouds. Thus the impact of the cloud inhomogeneity on the effective optical thickness should decrease as g increases to 1. Relation (22) does not satisfy exactly this limit condition $\Gamma(C_1, g) = 1$ as $g \to 1$, but this discrepancy has little numerical effect as long as g remains not too close to 1.

6.2. Contribution of the Total Optical Thickness

The global transmittance and reflectance of a cloud in the framework of the two-stream approximation is expressed as a function of both the asymmetry factor and total optical thickness for conservative scattering. Therefore we have to include the dependency of the effective optical thickness on the total optical thickness of the cloud into the above empirical relation. To keep a simple expression for the effective optical thickness, we assume that the dependency on τ_0 can be written as a multiplication factor of each term in (22)

$$\ln \Gamma(C_1, g) = -\left\{\frac{1 - g}{0.055 + 0.195(1 - g)}C_1F_1(\tau_0) + \left[0.9 - \frac{1 - g}{0.070 + 0.330(1 - g)}\right]C_1^2F_2(\tau_0)\right\} \quad (23)$$

This expression is fitted with the points computed for clouds with the total optical thickness varying from 0 to 80. Functions $F_1(\tau_0)$ and $F_2(\tau_0)$ are assumed to be quadratic with respect to τ_0:

$$F_1(\tau_0) = 0.30 + 0.04\tau_0 + 0.000239\tau_0^2 \quad (24a)$$

$$F_2(\tau_0) = -2.6 + 0.24\tau_0 + 0.0014\tau_0^2 \quad (24b)$$

The function $F_1(\tau_0)$ varies from 0.3 to about 2.5 as τ_0 changes from 0 to 80. The function $F_2(\tau_0)$ varies from -2.6 to about 7 for τ_0 from 0 to 80.

6.3. Empirical Expression of the Effective Optical Thickness as a Function of C_1, g, and τ_0

By summarizing all the adjustment and dependency examined above, we can write a final expression for the effective optical thickness. In doing so, we have to take account of the constraints given by (15) and other equations discussed above. This leads us to express the effective optical thickness τ' in the following form:

$$\tau' = [B(C_1, g, \tau_0) + \Gamma(C_1, g, \tau_0)\tau]\left[1 - \exp\left(-\frac{\tau}{AC_1}\right)\right] \quad (25)$$

where A is a constant. The first factor describes the linear dependency of the effective optical thickness on the original optical thickness of the inhomogeneous clouds, and the second factor describes the correction term effective in the range of small optical thickness. Data from simulations were fitted to this functional form, and the expressions $B(C_1, g, \tau_0)$ and $\Gamma(C_1, g, \tau_0)$ were determined as a function of C_1, g, and τ_0:

$$B(C_1, g, \tau_0) = \left\{\Gamma(C_1, g, \tau_0) + \frac{[2 - (2 - C_1)\Gamma(C_1, g, \tau_0)]}{2 + (1 - g)\tau_0}\right\}AC_1 \quad (26)$$

$$\Gamma(C_1, g, \tau_0) = \exp\{-[G_1(g, \tau_0)C_1 + G_2(g, \tau_0)C_1^2]\} \quad (27)$$

with

$$G_1(g, \tau_0) = \left[\frac{1 - g}{0.055 + 0.195(1 - g)}\right]F_1(\tau_0) \quad (28)$$

$$G_2(g, \tau_0) = \left[0.9 - \frac{1 - g}{0.070 + 0.330(1 - g)}\right]F_2(\tau_0) \quad (29)$$

where the functions $F_1(\tau_0)$ and $F_2(\tau_0)$ are given in (24).

6.4. Application of the Effective Optical Thickness in Two Stream Approximation

We estimated the transmittance and reflectance of inhomogeneous clouds by applying two-stream approximation to corresponding equivalent homogeneous clouds and using the equivalent optical thickness given by (25). These estimates were compared with those obtained for the same clouds with the DART model. Such a comparison can test the utility of the effective optical thickness in dealing with radiative properties of the inhomogeneous clouds and also evaluate globally the degree of adjustment of (25) established step by step.

We compared the global transmittance of the clouds whose data were not used for the adjustment of (25). These inhomogeneous clouds are of three types of the clouds with different sets of C_1 and g, ($C_1 = 0.1$, $g = 0.8$), ($C_1 = 0.2$, $g = 0.7$), and ($C_1 = 0.3$, $g = 0.6$), and a total optical thickness varying from 0 to 60. Figure 8a shows the relative difference for the global transmittance of the inhomogeneous clouds estimated from the equivalent optical thickness and two-stream approximation. This relative difference is less than about 3%. Figure 8b shows the relative difference for the same inhomogeneous clouds but without taking account of the cloud inhomogeneity. The bias between homogeneous and inhomogeneous transmittance increases with the total optical depth and C_1, and it may attain 150% for optically thick and very inhomogeneous clouds (Figure 8b). Thus much of the effect of heterogeneity can be captured by the introduction of the effective optical thickness in two-stream solutions.

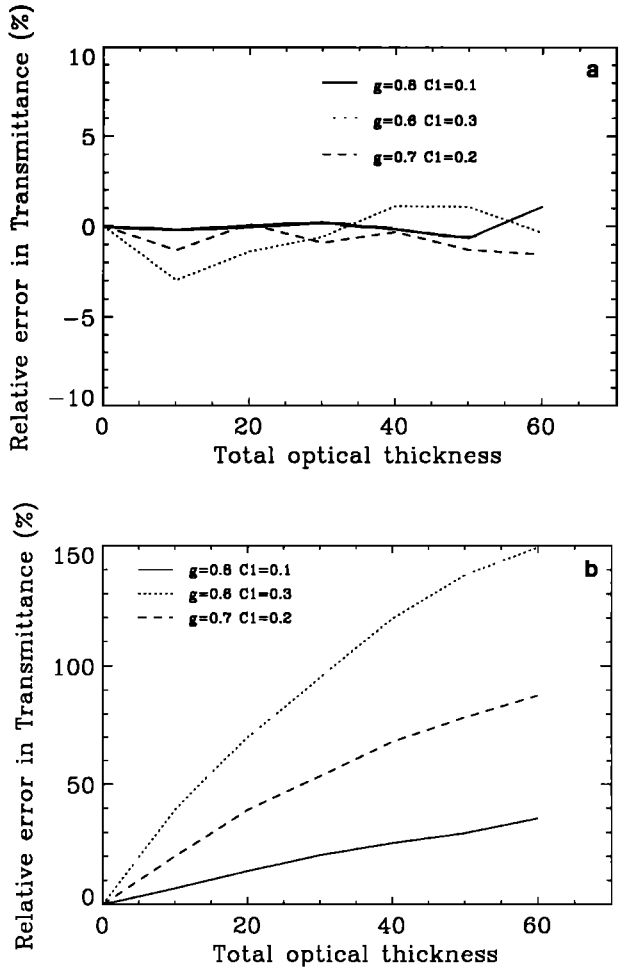

Figure 8. Comparison of the relative difference of the global transmittance of inhomogeneous clouds estimated from (25) with those obtained under the homogeneous cloud assumption. The inhomogeneous clouds are generated for total optical thickness varying from 0 to 60 with three sets of information codimensions and asymmetry factors: ($C_1 = 0.1$, $g = 0.8$), ($C_1 = 0.2$, $g = 0.7$), and ($C_1 = 0.3$, $g = 0.6$) (a) Relative difference between the global transmittances estimated from (25) and those estimated with the DART model as a function of the total optical thickness of the clouds for the three types of inhomogeneous clouds. (b) Relative difference between the global transmittances of the inhomogeneous clouds estimated under the homogeneous cloud assumption with those estimated with the DART model as a function of the total optical thickness for the same clouds as in Figure 8a.

7. Transmittance, Reflectance, and Absorption in Multifractal Absorbing Clouds

Figures 9a, 9b, and 9c present transmittance, reflectance, and absorptance as a function of ω_0 and C_1 for the inhomo-

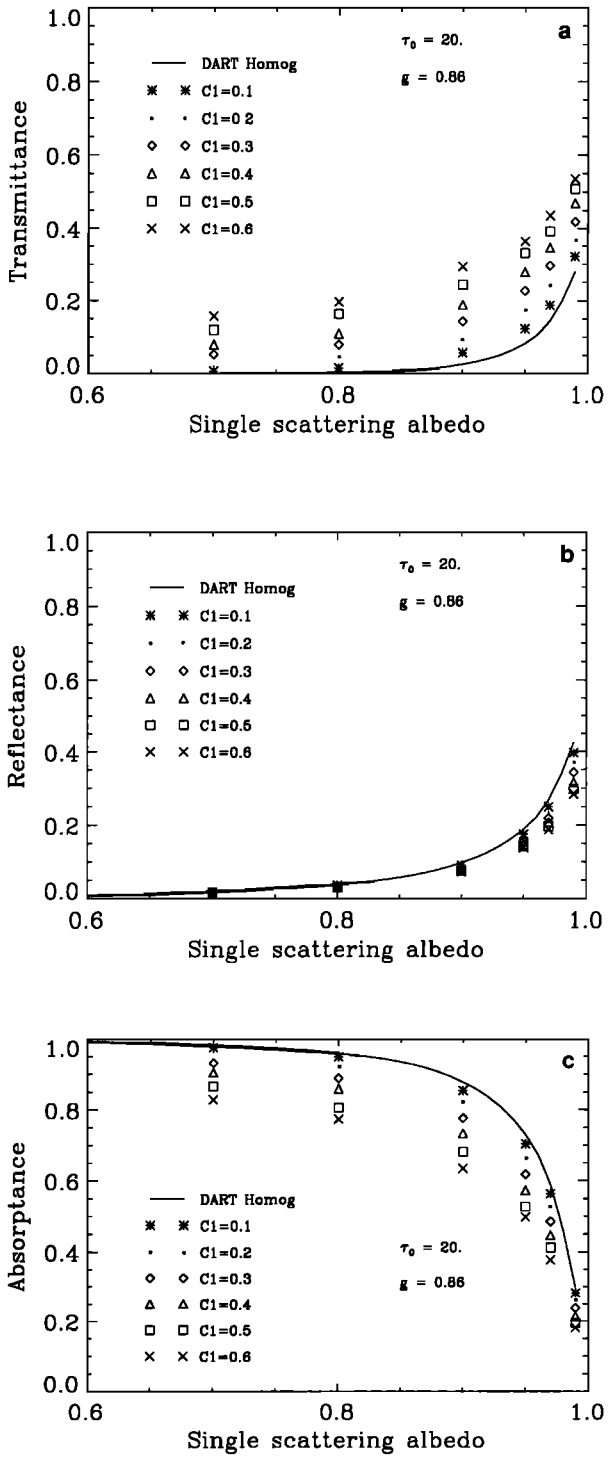

Figure 9. Variations of the (a) transmittance, (b) reflectance, and (c) absorptance of inhomogeneous clouds as a function of the single-scattering albedo ω_0 for different values of the information codimension C_1. The total optical thickness of the clouds and the asymmetry factor of the scatterers are kept constant at 20 and 0.86, respectively.

geneous clouds with $\tau_0 = 20$ and $g = 0.86$. We varied ω_0 from 0.7 to 0.99 and C_1 from 0 to 0.6.

The transmittance increases and the reflectance decreases as the cloud inhomogeneity increases from $C_1 = 0$ to $C_1 = 0.6$ (Figures 9a and 9b) for a fixed ω_0. These variations are qualitatively the same as those obtained for the nonabsorbing, inhomogeneous clouds. The transmittance of an inhomogeneous cloud increases by an extra transmittance that depends on C_1 and ω_0. For a given C_1 this increase is significantly larger for the interval $0.9 < \omega_0 < 0.97$ than outside it, but the magnitude of this increase does not exceed 15%. The effect of inhomogeneity on the reflectance differs significantly from the effect on the transmittance. It lessens rapidly as ω_0 decreases from 1 to 0.7, because the reflectance of a homogeneous cloud itself varies very rapidly with ω_0. The cloud inhomogeneity has a larger effect, in both absolute and relative value, on the transmittance than on the reflectance, but this feature may depend on the value of g.

As for the absorptance, an inhomogeneous cloud absorbs less energy than a homogeneous cloud with the same total mass of the scatterers (Figure 9c). As ω_0 decreases from 0.99 to 0.80, the absorptance increases from 0.23 to 0.95 for a homogeneous cloud and from 0.18 to 0.78 for an inhomogeneous cloud with a C_1 of 0.6. Hence the absorptance of highly inhomogeneous clouds with a moderate optical thickness is smaller than that of the corresponding homogeneous clouds by 20 to 30%. These features are due to the fact that increasing inhomogeneity enlarges the area with small local optical thickness through which light is preferentially transmitted and reduces the area with large local optical thickness from which light is preferentially reflected.

Figures 10a, 10b, and 10c present the variation of the transmittance, reflectance, and absorptance as a function of the single-scattering albedo for the inhomogeneous clouds with the same characteristics as in Figure 1, but with a total optical thickness of 80. The transmittance and reflectance (Figure 10a and 10b) show variations with the cloud inhomogeneity similar to those in Figure 9a and 9b. The transmittance still changes significantly with the cloud inhomogeneity for a ω_0 close to 1, while its variation with C_1 lessens rapidly in amplitude for ω_0 less than 0.9. This feature differs from that observed above for the clouds with a total optical thickness of 20.

The reflectance from the clouds with $\tau_0 = 80$ does not differ from that obtained for the clouds with $\tau_0 = 20$. This suggests that the energy is reflected by the upper part of the cloud whose optical thickness is less than 20. Therefore adding more absorbing scatterers does not affect the amount of reflected energy. An optically very thick cloud absorbs almost all nonreflected energy, except in the case with ω_0 very close to 1. As ω_0 decreases from 0.99 to 0.80, the absorptance increases from 0.48 to 0.97 for a homogeneous cloud and from 0.36 to 0.93 for an inhomogeneous cloud with a C_1 of 0.6. Hence moderate to high cloud inhomogeneity generally reduces the absorptance from its homogeneous cloud value. However, the magnitude of the effect is much smaller than the previous case ($\tau_0 = 20$), except for a ω_0 very close to 1. This implies that cloud inhomogeneity is not a pertinent physical factor for the reflectance for a highly absorbing cloud.

A close examination of Figure 10c shows that the absorptance of an inhomogeneous cloud with a small C_1 ($C_1 < 0.2$) is equal to or slightly higher than the absorptance of a homogeneous cloud with the same optical characteristics. This feature is quite different from that obtained for the same inhomogeneous clouds with a smaller total optical thickness of 20.

The conservation of the energy derives the expressions

$$A_{\text{hom}} = 1 - [T_{\text{hom}}(\omega_0, g) + R_{\text{hom}}(\omega_0, g)] \qquad (30a)$$

$$A_{inh} = 1 - [T_{inh}(\omega_0, g, C_1) + R_{inh}(\omega_0, g, C_1)]$$

$$= A_{hom} - [\delta T_{inh}(\omega_0, g, C_1) + \delta R_{inh}(\omega_0, g, C_1)] \quad (30b)$$

where A_x, T_x, and R_x are the absorptance, transmittance and reflectance of the cloud, respectively, the index x designating the homogeneous (hom) or inhomogeneous (inh) cloud.

Figures 11a, 11b, and 11c show the relative difference, defined by $(A_{hom} - A_{inh})/A_{hom}$, of the absorptance between inhomogeneous and homogeneous clouds with total optical thickness of 20, 50, and 80, respectively.

For moderate and large cloud inhomogeneity ($C_1 > 0.2$), the relative difference generally increases as ω_0 approaches to 1. A highly intermittent inhomogeneous cloud ($C_1 > 0.4$) absorbs 10–40% less energy than a homogeneous cloud for $\tau_0 = 20$ and 5–30% less for $\tau_0 = 80$), while a slightly or moderately inhomogeneous cloud ($0.2 < C_1 < 0.4$) absorbs 5–20% less energy for $\tau_0 = 20$ and 2–10% less for $\tau_0 = 80$). The relative difference increases with ω_0 because the decrease of the absorptance is large enough to compensate the lessening inhomogeneity effect as ω_0 approaches 1.

For the inhomogeneous clouds with C_1 smaller than 0.2, the cloud inhomogeneity tends to increase systematically the absorptance of the clouds with a total optical thickness larger than 50 and ω_0 larger than 0.85. However, the increase is less than 5%, much smaller than expected. This result agrees with that obtained by *Barker* [1992] for monofractal clouds with a total optical thickness larger than 40. This increase happens because the cloud inhomogeneity enables photons to penetrate deeper into the clouds, but these photons cannot come out from the clouds owing to the large optical thickness and are finally absorbed into the clouds.

For a cloud with a small to moderate optical thickness ($\tau_0 < 30$) the effect of inhomogeneity on the transmittance is larger than that on the reflectance (Figures 12a and 12b), so the sum $\delta T_{inh} + \delta R_{inh}$ is always positive. Consequently, the absorptance of an inhomogeneous cloud is always smaller than that of a homogeneous cloud with the same total optical thickness.

For an optically thick cloud with a total optical thickness ($\tau_0 > 50$), the situation becomes more complicated. The cloud inhomogeneity always decreases the reflectance. However, the reflectance of an optical thick cloud does not differ very much from that of a cloud with an optically moderate thickness because the energy is reflected mostly by the upper part of the cloud. Nonreflected energy penetrates into the cloud, but the transmittance rapidly approaches zero for a weakly inhomogeneous cloud with ω_0 less than 0.95. Consequently, the nonreflected energy is trapped into the cloud and is finally absorbed by the cloud scatterers. In this case, we have the sum $\delta T_{inh} + \delta R_{inh}$ negative, which corresponds to the increased absorptance. For an inhomogeneous cloud with a large C_1, the inhomogeneity effect allows a small amount of the energy to still be transmitted through the cloud, and this effect remains larger than the negative effect on the reflectance. Therefore the sum $\delta T_{inh} + \delta R_{inh}$ remains positive, and the absorptance decreases because of the cloud inhomogeneity. Radiative fluxes are computed again for the same clouds, but with larger total optical thickness $\tau_0 = 80$ (Figure 11c). Results show that the absorptance of an inhomogeneous cloud can be larger than the absorptance of a homogeneous cloud with the same optical thickness by 5%. Therefore how the cloud inhomogeneity affects the radiative properties of a cloud depends not only on the scattering properties of the scatterers and the total optical thickness of the cloud, but also on the characteristics of the inhomogeneity. Hence we have to be careful to generalize this result for all types of inhomogeneous clouds because the multifractal medium has a very specific distribution of fluctuations.

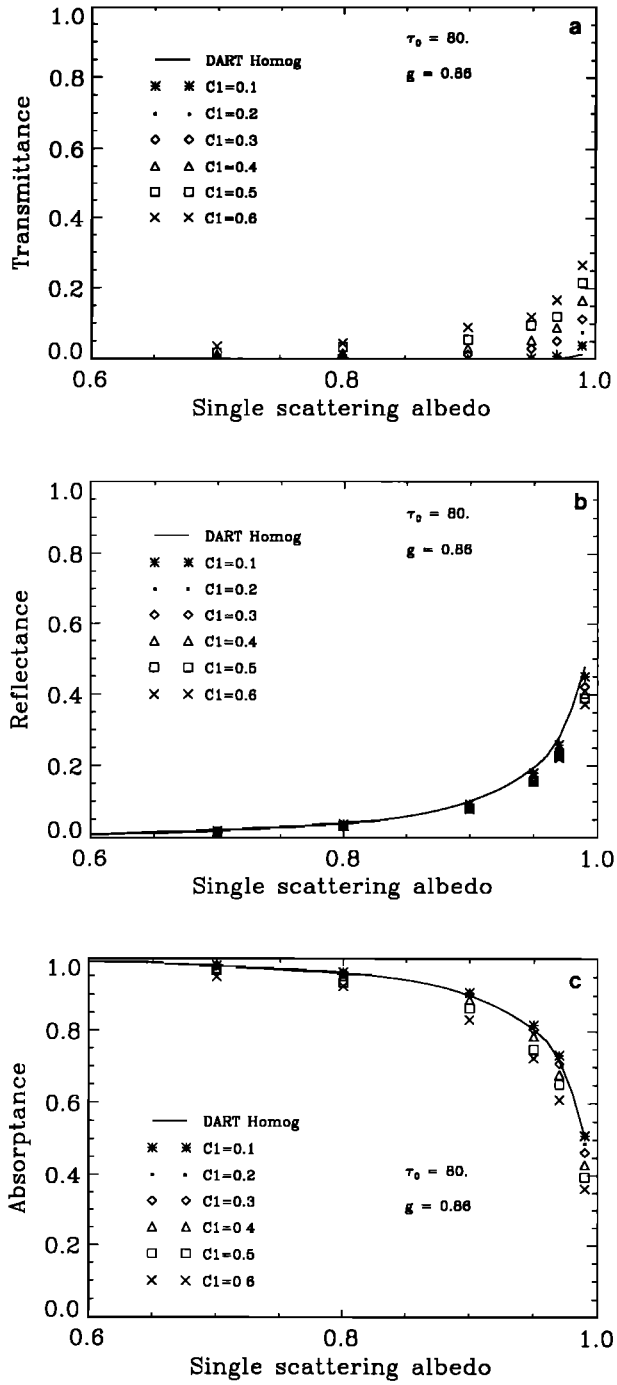

Figure 10. The same as Figure 9, but for a total optical thickness of 80.

8. Application of the Effective Optical Thickness to Inhomogeneous Absorbing Clouds

For nonconservative scattering we have defined an effective optical thickness for inhomogeneous clouds as a function of

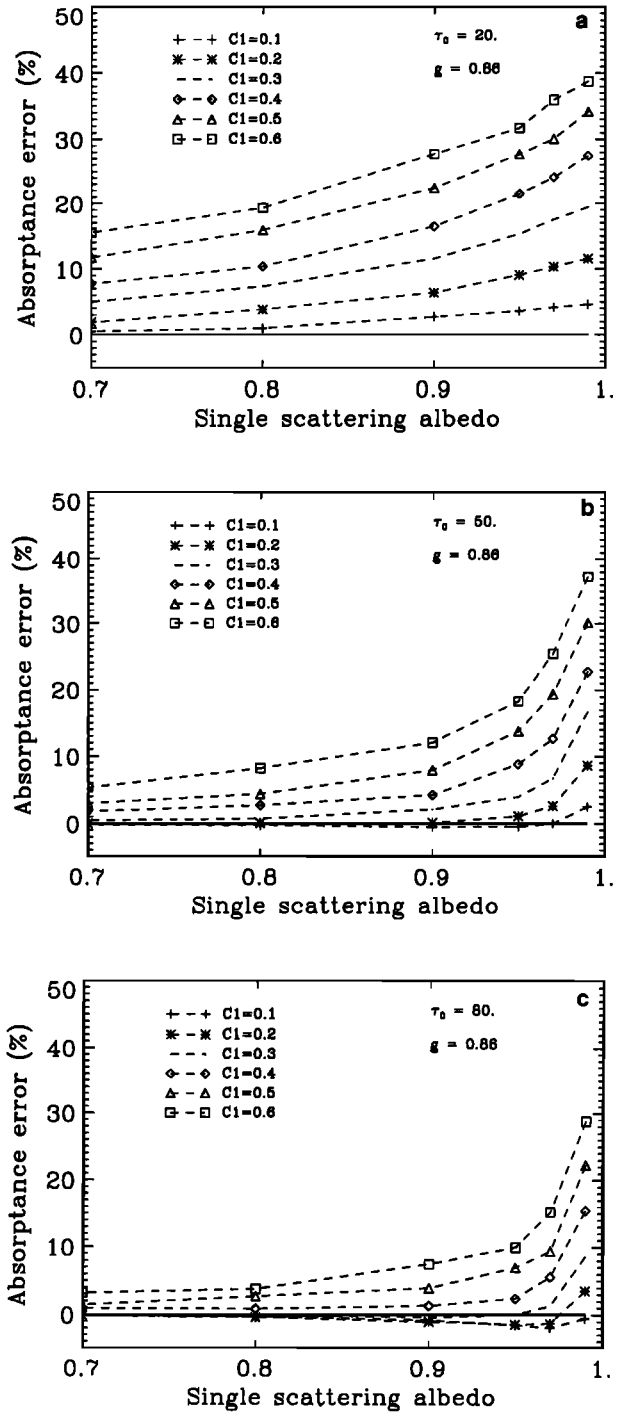

Figure 11. Variations of the relative difference of the absorptance $(A_{\text{hom}} - A_{\text{inh}})/A_{\text{hom}}$ between homogeneous and inhomogeneous clouds as a function of the single-scattering albedo ω_0 for different values of the information codimension C_1 and optical thickness of (a) 20, (b) 50, and (c) 80. A_{hom} and A_{inh} designate the absorptance of a homogeneous cloud and corresponding inhomogeneous cloud, respectively. The total optical thickness of the clouds and the asymmetry factor of the scatterers are kept constant at 20 and 0.86, respectively.

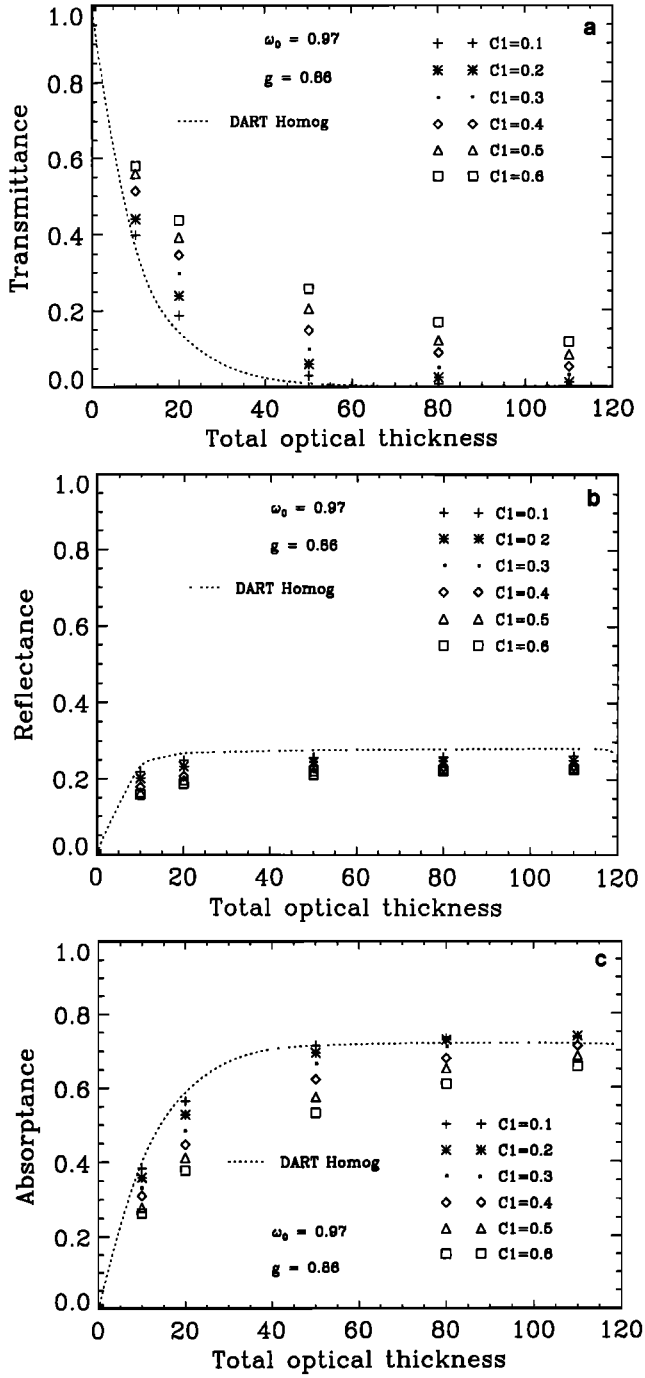

Figure 12. Variations of the (a) transmittance, (b) reflectance, and (c) absorptance of inhomogeneous clouds as a function of the total optical thickness τ_0 for different values of the information codimension C_1. The dashed line corresponds to the homogeneous cloud. The single-scattering albedo and the asymmetry factor of the scatterers are kept constant at 0.97 and 0.86, respectively.

the C_1, g, and τ_0 and transformed the estimation of the radiative flux in the inhomogeneous cloud into that in an equivalent homogeneous cloud. Can we apply the same approach to inhomogeneous, absorbing clouds? The effective optical thickness we have defined for the inhomogeneous, nonabsorbing clouds may be considered as weighted average of local optical thickness over an inhomogeneous cloud layer with an average optical depth ($\tau \leq \tau_0$). Because the scatterers have been assumed to be nonabsorbing, the effective optical thickness defined in (25) takes into account only effects of the cloud inhomogeneity on the scattering. For the absorbing scatterers we

need to consider effects of the cloud inhomogeneity on both the scattering and absorption, since the cloud inhomogeneity may affect the scattering and absorption in different ways.

There are many possible options to define an effective optical thickness for the absorbing clouds. The first one is to consider two distinct effective optical thickness, one similar to that defined in (25) for the scattering part, and the other one for the absorption part of the average optical thickness. We did not adopt such an approach for two reasons. Such a definition will result in too cumbersome expressions. Moreover, it will be difficult to separate an experimentally measured optical thickness into these two distinct parts. The second option is to define an effective optical thickness from an equivalent homogeneous absorbing cloud based on a delta-Eddington approximation. We could adopt this definition if the radiative properties of homogeneous clouds estimated with a two-stream approximation agreed well with those estimated with the DART model. However, we found small but systematic biases between the DART model and delta-Eddington approximations which make the error analysis of the results difficult. The third option is to adopt the effective optical thickness defined in (25) and to define a correction term on ω_0 if necessary. The use of the effective optical thickness defined in (25) assumes that the inhomogeneity has the same effect on both the scattering and absorption. In spite of this ad hoc assumption, we preferred to try this definition because of its simplicity.

Figures 13a, 13b and 13c show the same radiative parameters, presented in Figure 12, as a function of the effective optical thickness τ_0'. The most remarkable difference between Figures 12 and 13 is that all the dispersed points in Figure 12 are gathered along the corresponding homogeneous cloud curves in Figure 13, which shows that the cloud inhomogeneity effect is almost entirely accounted for by the effective optical thickness. The same feature can also be observed in Figure 14, which is identical to Figure 13 but corresponds to $\omega_0 = 0.9$. These figures confirm the above observation that the effective optical thickness makes it possible, from the practical point of view, to deal with the inhomogeneous cloud problem as the homogeneous cloud problem. Nevertheless, we can see some systematic difference between two DART estimations, one for the inhomogeneous clouds and the other for the equivalent homogeneous clouds.

The transmittance of the equivalent homogeneous clouds is slightly larger than that of the inhomogeneous clouds; when the clouds have a large cloud intermittency ($C_1 > 0.5$) and a total optical thickness larger than 50, the difference may reach 0.05. As for the absorptance, the inhomogeneous cloud points are distributed around the homogeneous cloud curve for $\omega_0 = 0.97$. Their departure from the homogeneous cloud curve is larger for $\omega_0 = 0.9$ than for $\omega_0 = 0.97$, but it remains less than 0.05. The reflectance of the equivalent homogeneous clouds always overestimates the reflectance of the inhomogeneous cloud, particularly for C_1 larger than 0.5. For $\omega_0 = 0.9$ the reflectance of the homogeneous clouds itself is small, and consequently the difference is small.

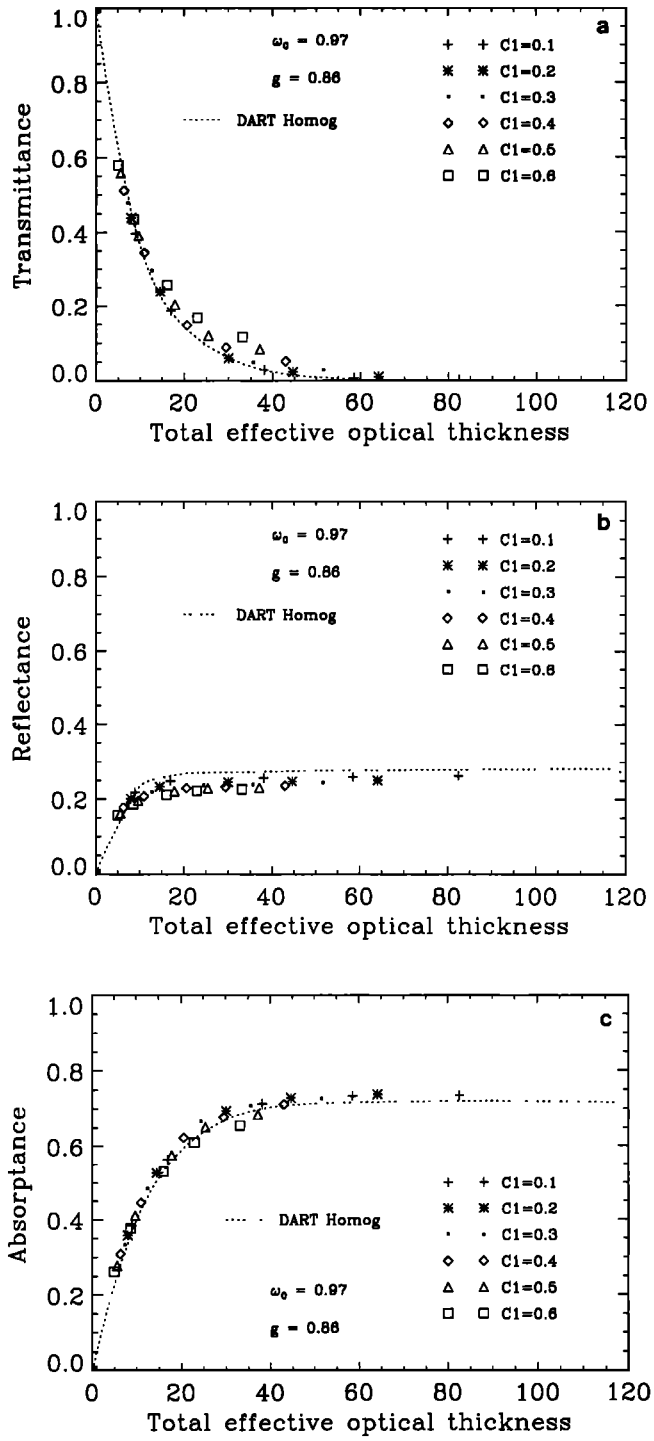

Figure 13. Variations of the (a) transmittance, (b) reflectance, and (c) absorptance of inhomogeneous clouds as a function of the total effective optical thickness for different values of the information codimension C_1. The dashed line corresponds to the homogeneous cloud. The single-scattering albedo and the asymmetry factor of the scatterers are kept constant at 0.97 and 0.86, respectively.

9. Use of the Effective Optical Thickness in Two-Stream Approximations

We have seen above that the effective optical thickness allows us to treat an inhomogeneous cloud as a homogeneous cloud and to improve significantly the estimation of its optical and radiative properties. In doing so, we compared the radiative flux in the inhomogeneous clouds with the flux in the equivalent homogeneous clouds calculated with the DART model, because of systematic bias between the DART model and typical two-stream approximations. In this section we examine how worthwhile it is to use the effective optical thickness

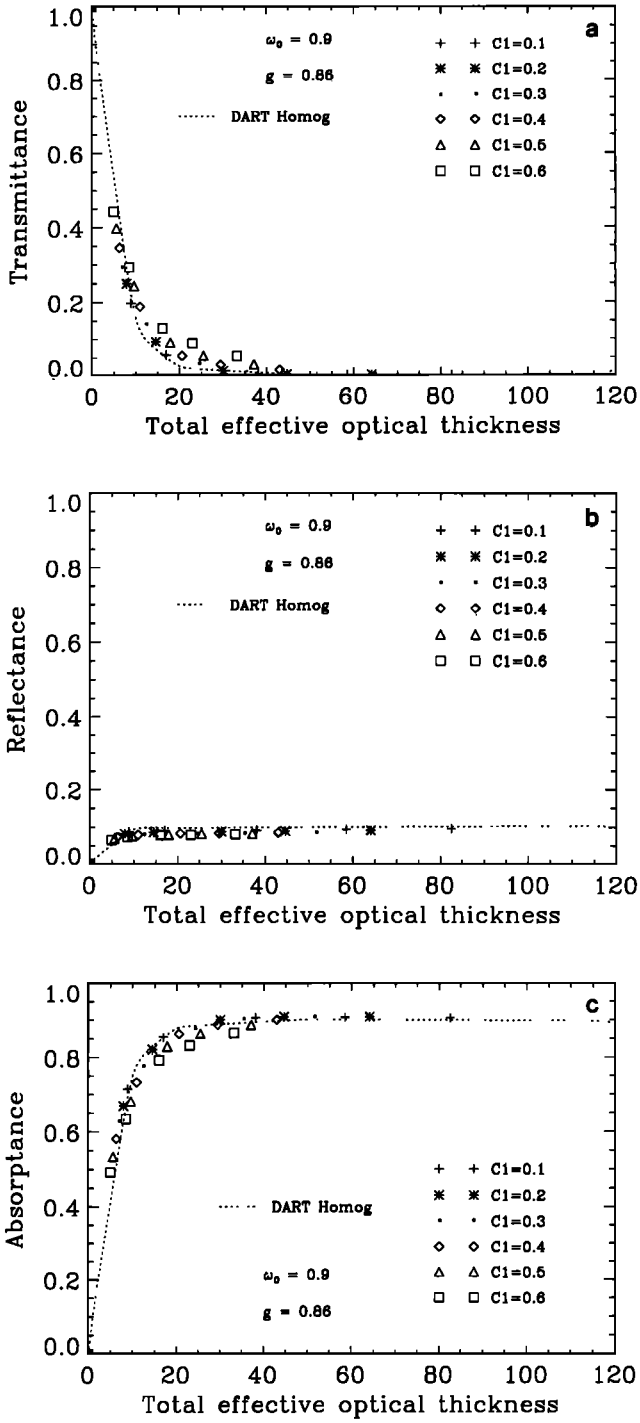

Figure 14. The same as Figure 13, but for a single-scattering albedo of 0.9.

in these typical radiative transfer approximations. According to *Meador and Weaver* [1980], the transmittance T and reflectance R of a homogeneous layer with an optical thickness equal to τ_0, can be expressed by

$$T = \frac{2k \exp(-k\tau_0)}{k + \gamma_1 + (k - \gamma_1)\exp(-2k\tau_0)}$$
$$R = \frac{\gamma_2[1 - \exp(-2k\tau_0)]}{k + \gamma_1 + (k - \gamma_1)\exp(-2k\tau_0)} \quad (31)$$

with

$$k = (\gamma_1^2 - \gamma_2^2)^{1/2}$$

where the quantities γ_1 and γ_2 depend on the type of the approximation. They vary with g, ω_0, and other parameters but do not depend on the total optical thickness τ_0 of the layer. These expressions are established with the boundary conditions at the upper and lower surface: $I\downarrow(0) = F\mu_0$ and $I\uparrow(\tau_0) = 0$, where F is the incident flux per unit area perpendicular to the propagation direction defined by μ_0 and τ_0. We selected the delta-Eddington approximate solutions [*Joseph et al.*, 1976]. The quantities γ_1 and γ_2 are expressed as follows:

Delta-Eddington approximation

$$\gamma_1 = \frac{7 - 3g^2 - \omega_0(4 + 3g) + \omega_0 g^2(4\beta_0 + 3g)}{4[1 - g^2(1 - \mu_0)]}$$
$$\gamma_2 = \frac{1 - g^2 - \omega_0(4 - 3g) - \omega_0 g^2(4\beta_0 + 3g - 4)}{4[1 - g^2(1 - \mu_0)]} \quad (32)$$

The term β_0 represents the global backscattering coefficient defined by

$$\beta_0 = \int_0^1 \int_0^1 P(-\mu'; \mu)\, d\mu'\, d\mu \quad (33)$$

where $P(-\mu'; \mu)$ represents the scattering phase function.

From the conservation of the energy, the absorptance of the cloud is given by the expression $A = 1 - (T + R)$. For an optically thick cloud we have limiting values

$$T(\tau_0 \to \infty) = 0$$
$$R(\tau_0 \to \infty) = \frac{\gamma_2}{k + \gamma_1} \quad (34)$$
$$A(\tau_0 \to \infty) = 1 - \frac{\gamma_2}{k + \gamma_1}$$

We calculated the transmittance, reflectance, and absorptance with the DART model, discrete ordinate method (DOM) [*Iaquinta*, 1996] and delta-Eddington approximation, as a function of the total optical thickness τ_0 for the homogeneous plane parallel clouds. The single-scattering albedo was taken equal to 0.97 and 0.9, and the asymmetry factor of the scatterers was of 0.86. Results are plotted in Figure 15 (ω_0 = 0.97) and Figure 16 (ω_0 = 0.9). The largest relative difference between these two models does not exceed 8% (Figure 15) for the absorptance, reflectance, and transmittance. DART results agree better with those computed with the discrete ordinate method, especially in the case of low single-scattering albedo (Figure 16), than with the delta-Eddington approximation results. The larger difference remarked between these the DART and DOM results in Figure 16 may be explained because when ω_0 approaches 1, the number of iterations increases considerably for the evaluation of multiple scattering, as well as the unavoidable numerical errors (particularly in the DOM).

Although the delta-Eddington approximation may sometimes produce nonphysical results [*Welch and Zdunkowski*, 1982], it remains the most frequently used radiative transfer model, and so we compare its results with the DART results in more detail. It is well known that the classical Eddington ap-

proximation is not adapted to a large asymmetry factor ($g > 0.6$). The delta-Eddington approximation remedies this fault and improves the flux estimation over a large range of applicability: $0.7 < \omega_0 < 0.99$ and $0 < g < 0.95$ [*Joseph et al.*, 1976]. Consequently, it is not surprising that the delta-Eddington approximation behaves as a good approximation of the DART model, in spite of some characteristic differences in the range of moderate and large optical thickness (Figures 15 and 16). The transmittance exhibits quite similar variations with optical thickness for both the methods. The discrepancy between two transmittances is larger for $\omega_0 = 0.9$ than for $\omega_0 = 0.97$. However, since the slope is highly negative for $\omega_0 = 0.9$, a large difference in the transmittance corresponds only to a very small variation of the optical thickness (less than 1.0).

The absorptance and reflectance vary in almost identical ways for both the methods. The delta-Eddington approximation slightly underestimates the absorptance and overestimates the reflectance in the range of large optical thickness ($\tau_0 > 30$ in Figure 15 and $\tau_0 > 20$ in Figure 16). However, the difference between the DART model and delta-Eddington does not exceed 0.03 in absolute value for both the absorptance and reflectance. So, delta-Eddington approximation can be considered as a reasonable approximation to the DART model in computing the radiative fluxes through homogeneous clouds, except clouds with a reflectance less than 0.2, for which a bias of 0.03 represents a relative error of more than 10%. The relative error on the absorptance is generally less than that for the reflectance. For example, for $\omega_0 = 0.97$ the relative error on the absorptance is about 2.6% for an optically thick cloud and less than 4% in an optically thin cloud. For more absorbing scatterers ($\omega_0 < 0.9$), the limits of errors become 3.5% and 7%, respectively.

In the preceding section we showed that the introduction of the effective optical thickness in the DART model enables to treat an inhomogeneous cloud as a equivalent homogeneous plane parallel cloud despite some minor discrepancy. This finding, combined with the result for the delta-Eddington approximation, suggests that we can use the delta-Eddington approximation with the effective optical thickness to improve

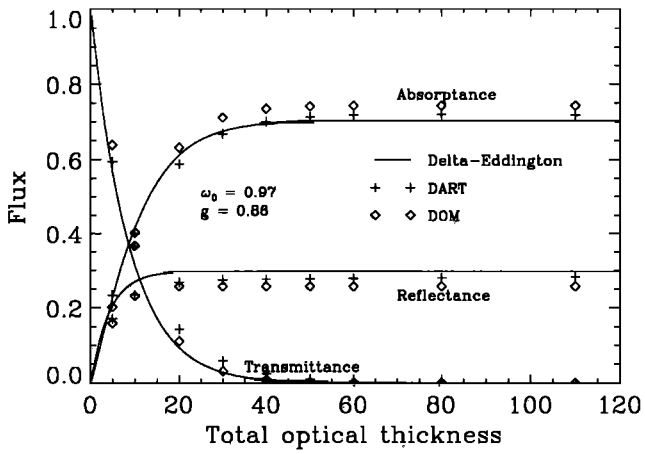

Figure 15. Comparison between the delta-Eddington approximation, DOM, and DART results of the transmittance, reflectance, and absorptance of homogeneous clouds as a function of the total optical thickness τ_0. The single-scattering albedo and the asymmetry factor of the scatterers are kept constant respectively at 0.97 and 0.86.

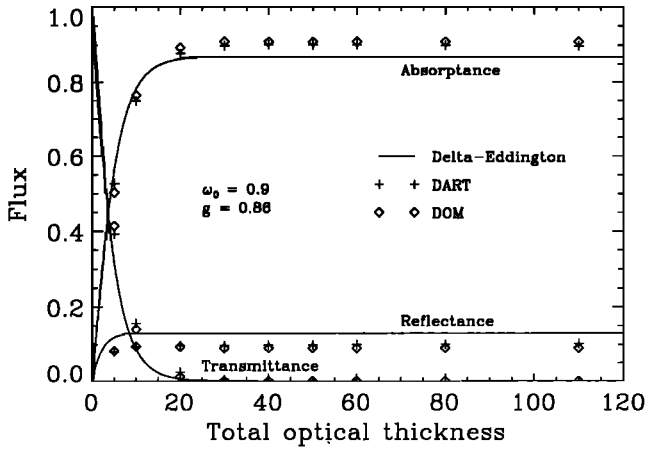

Figure 16. The same as Figure 15, but for a single-scattering albedo of 0.9.

significantly the estimation of the radiative fluxes of an inhomogeneous cloud. If we calculate the reflectance and absorptance of an inhomogeneous cloud as for a homogeneous cloud, the relative error would be greater than 60% for highly inhomogeneous clouds. The use of the effective optical thickness in the delta-Eddington approximation may diminish this error less than 10% in most of the conditions. Moreover, this errors in the flux estimation should be mainly due to the systematic bias between the DART model and delta-Eddington approximation.

10. Comparative Analysis With Independent Pixel Approximation

Cahalan [1989], *Cahalan et al.* [1994a, b] and *Marshak et al.* [1995] have considered the impact of cloud heterogeneity on radiative transfer, based on independent pixel approximation (IPA), in which the reflectivity of each cloud pixel depends only on its own optical thickness and not on the optical thickness of neighboring pixels. An average reflectance of inhomogeneous clouds was defined by taking account of spatial fluctuations of the optical thickness. For the comparison of DART- and IPA-based effective optical thickness, we need to transform the DART results into the IPA framework.

Figures 17a and 17b show the transmittance and reflectance, respectively, calculated with the DART model and IPA model (upper curves), and the difference (lower curves). We simulated two clouds of 512 × 512 pixels with $\tau_0 = 20$, $g = 0.86$, and $\omega_0 = 0.99$ but with different values of C_1 (0.1 in Figure 17a and 0.3 in Figure 17b). In the IPA model, the reflectance and transmittance of each columns are estimated by applying the classical two-stream approximation formula proposed by *Meador and Weaver* [1980] on vertically integrated optical thickness for each column. Differences between the IPA and DART results should occur in regions where the optical thickness of columns differs significantly from the ones of neighboring columns. (We can see that this difference reaches a value of 0.2 for both transmittance and reflectance.) In these regions the IPA tends to underestimate the reflectance, while for optically thin or relatively uniform regions the DART and IPA results agree fairly well, as expected.

A variance parameter f is defined as the variance of the logarithm of the cloud liquid water path W. According to

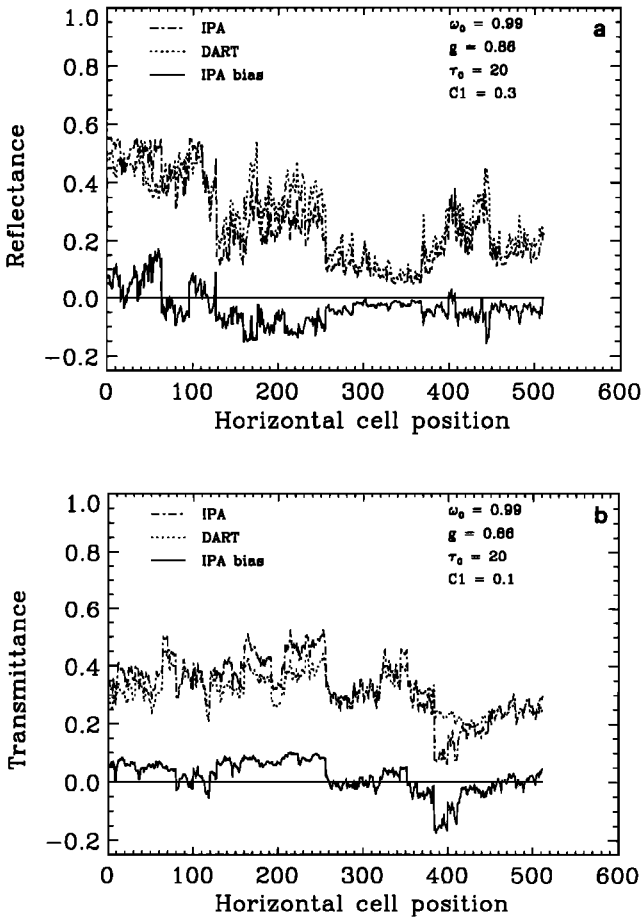

Figure 17. Comparison of DART and IPA transmittance, 17a, and reflectance, 17b in two 2-D heterogeneous clouds which have respectively an information codimension equals to 0.1 (Figure 17a) and 0.3 (Figure 17b). Lower curve shows the absolute difference between DART and IPA results.

Cahalan et al. [1994a, b] and *Marshak* [1995], this parameter varies with the seasons, time of day, and cloud type. A value of about 0.39 is reported for marine stratocumulus. For 1-D lognormal multiplicative model f can be theoretically expressed as a function of C_1 by

$$f = 2C_1 \ln (L/r) \tag{35}$$

where r and L are the observation and external scales. Unfortunately, there is no simple analytical expression relating the parameter f to the information codimension C_1 of 2-D multifractal fields. Hence we estimated f from the water path W vertically integrated for each column of the 2-D multifractal clouds, as a function of C_1. Figure 18 shows the mean and first through and third quartiles of the histogram of f determined from 50 realizations. The respective location of these statistical parameters indicates the histogram is positively skewed. We may nevertheless fit the mean with a linear expression. From this empirical curve we can estimate an information codimension of $C_1 \approx 0.22$ corresponding to the parameter $f \approx 0.39$ evaluated by *Cahalan et al.* [1994a] for real marine stratocumulus.

Figure 19 shows the DART- and IPA-based effective optical thicknesses of 2-D heterogeneous clouds with $\tau_0 = 20$, $\omega_0 = 0.99$, and $g = 0.86$, as a function of C_1. The DART-based

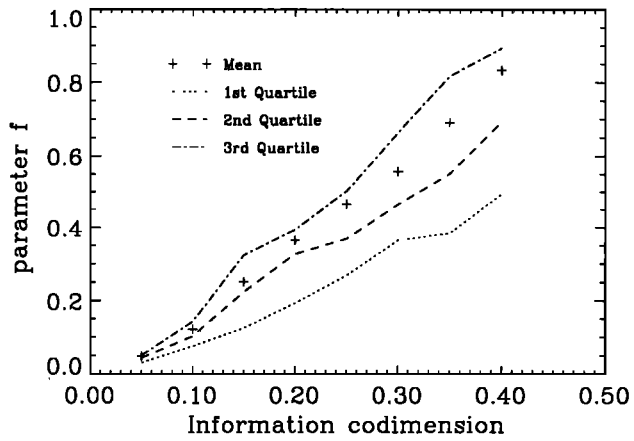

Figure 18. Variance parameter f of vertically integrated 2-D heterogeneous field as a function of the 2-D information codimension. Mean and quartiles are estimated from 50 realizations.

effective optical thickness from this study, $\tau_{B\&I}$, is calculated from (25), and the IPA-based effective optical thickness τ_{Cah} is evaluated from Cahalan's expression [*Cahalan et al.*, 1994a]

$$\tau_{Cah} = \chi \tau_0 \tag{36}$$

where the "reduction factor" χ is expressed as a function of the variance parameter f and cascade step by

$$\chi = \left(\prod_{n=0}^{\infty} (1 - f^2) \right)^{1/2}. \tag{37}$$

Figure 19 shows significantly different behaviors of the two effective optical thicknesses with the 2-D information codimension C_1. Consequently, the radiative properties of the corresponding "equivalent plane parallel" clouds should also differ considerably. The IPA based effective optical thickness τ_{Cah} decreases very rapidly with the heterogeneity in comparison with $\tau_{B\&I}$. This difference is a consequence of the vertical heterogeneity in the 2-D lognormal multiplicative fields. We need a further investigation, however, to evaluate the effect of

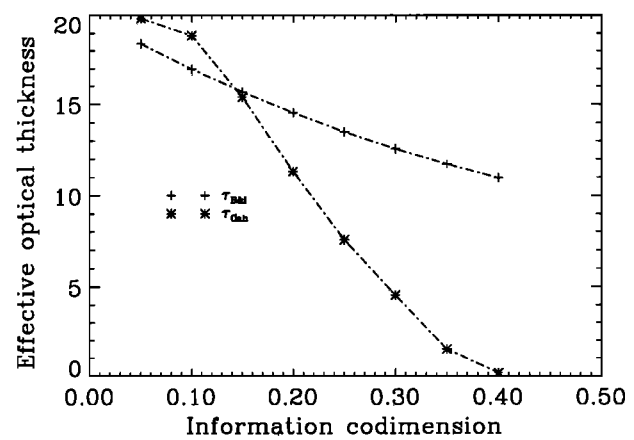

Figure 19. Variation of the IPA-based (τ_{Cah}) and DART-based ($\tau_{B\&I}$) effective optical thicknesses of heterogeneous clouds ($\tau_0 = 20$, $g = 0.86$, $\omega_0 = 0.99$) as a function of the 2-D information codimension C_1.

vertical inhomogeneity on the radiative properties of natural clouds.

11. Summary and Conclusion

The objective of this study was to investigate relationships between radiative properties of inhomogeneous and homogeneous clouds by using the DART model and 2-D multifractal clouds. It was shown that inhomogeneous clouds transmit more radiation energy than their homogeneous counterparts in the hypothesis of conservative scattering, because the direct transmission of light is favored through optically less dense area of the cloud and this overcompensates lesser direct transmission in optically denser area of the cloud. To quantify the nonlinear effect of inhomogeneity, we defined an effective optical thickness of inhomogeneous clouds in the framework of the two-stream approximation and plane parallel homogeneous clouds.

A semiempirical relation for the effective optical thickness was established as a function of the information codimension C_1, total optical thickness, τ_0, and asymmetry factor g of the scatterer by step by step fitting. It should be valid for an inhomogeneous cloud with a C_1 parameter ($0 < C_1 < 0.6$), a total optical thickness ($0 < \tau_0 < 80$) and an asymmetry factor ($0 < g < 1$). For 2-D clouds with nonabsorbing scatterers, we showed that the introduction of this effective parameter into the two-stream equations enables calculation of the global transmittance and reflectance with a relative error less than 5%.

This paper presents also an investigation on the impact of the cloud heterogeneity on the absorption process. We showed that an inhomogeneous cloud absorbs generally less radiation than its homogeneous counterpart for an optically thin or moderate cloud. However, for an optically thick cloud an inhomogeneous cloud can absorb more energy than its homogeneous counterpart when the degree of inhomogeneity of the cloud is not too high and its optical thickness is high enough. The inhomogeneity tends to decrease the albedo at the top of the cloud, while the high optical thickness does not allow the energy that has penetrated to leave the cloud. The limit between these two behaviors depends on C_1, ω_0, and g. Although this effect is smaller than expected, this finding may provide an explanation for anomalous cloud absorption [*Stephens and Tsay*, 1990]. In spite of residual biases, we have shown too that the use of the effective optical thickness in the delta-Eddington equations gives a fairly good evaluation of the transmittance, reflectance, and absorptance of an inhomogeneous absorbing cloud.

Many problems have been left outside the limited scope of the present study. We need to look into the eventual difference of effects of the inhomogeneity on the absorption and scattering, which may lead to modifying the definition of the effective optical thickness.

One of the main problems in both the climate modeling and the processing of satellite data is how to integrate effects of subgrid-scale or subpixel-scale inhomogeneities of the clouds and cloud fields in the cloud parametrization and/or retrieval of cloud characteristics. The present results show a possibility of transforming some radiative transfer problems in inhomogeneous clouds into those in equivalent homogeneous clouds, even if it is far from providing reliable solutions to the above questions. We have shown that for two-dimensionally inhomogeneous clouds the DART-based effective optical thickness differs considerably from the IPA-based effective optical thickness proposed by *Cahalan et al.* [1994a].

In this study we used multifractal clouds because their intermittency is entirely defined by the information codimension. We intentionally adopted the simplest representation that is available to generate a multifractal field in spite of the unnaturalness of such a field to represent natural cloud inhomogeneity on subcloud scales. *Schertzer and Lovejoy* [1991], *Tessier et al.* [1993], and *Marshak et al.* [1994] proposed methods of multifractal analysis to process satellite pictures and/or "in situ" microphysical data and estimate the C_1 parameter and the other multifractal parameter H_1. Therefore the present investigation needs to be extended to other inhomogeneity generation processes.

We have to emphasize the need for reliable statistical methods and parameters to describe inhomogeneous structure of the clouds. Indeed, we could develop the above approach and define the effective optical thickness of the inhomogeneous clouds, because the inhomogeneous structure of the cloud was characterized only by the C_1 parameter. This parameter integrates at least two distinct information contents about the inhomogeneity of the cloud, the one on the amplitude of fluctuations and the other on the spatial correlation of fluctuations as discussed above. The results of our present study do not give any indication about which of these inhomogeneity characteristics is pertinent to the effective optical thickness we have defined. Answers to this question may have important impact on the processing of experimental data, because we do not have well-established methods for processing these data. There is a urgent need for a better understanding of what heterogeneity characteristics are relevant to the radiative transfer in inhomogeneous clouds.

All these approaches are based on an empirical adjustment of simulation data without any detailed theoretical analysis of the radiative transfer equation. It is now evident that the present empirical approach should be put on a more solid theoretical basis. In this study we discussed only the radiative flux in a very simple situation of vertical illumination. This approach also has to be extended to consider the angle of incident light and also to examine effects of cloud inhomogeneity on the bidirectional reflectance. These problems need to be investigated in relation to the integration of the inhomogeneity effect in procedures of retrieval of the cloud characteristics from satellite measurements.

References

Aida, M., Scattering of solar radiation as a function of cloud dimensions and orientation, *J. Quant. Spectrosc. Radiat. Transfer*, *17*, 303–310, 1977.

Barker, H. W., Solar radiative transfer through clouds possessing isotropic variable extinction coefficient, *Q. J. R. Meteorol. Soc.*, *118*, 1145–1162, 1992.

Brenguier, J. L., Parameterization of the condensation process in small nonprecipitating cumuli, *J. Atmos. Sci.*, *47*, 1127–1148, 1990.

Bréon, F. M., Reflectance of broken cloud fields: Simulation and parameterization, *J. Atmos. Sci.*, *49*, 1221–1232, 1992.

Cahalan, R. F., Overview of fractal clouds, in *Advances in Remote Sensing Retreval Methods*, edited by A. Deepak, H. Flemming, and J. Theon, pp. 371–388, A. Deepak, Hampton, Va., 1989.

Cahalan, R. F., W. Rigdway, W. J. Wiscombe, T. L. Bell, and J. B. Snider, The albedo of fractal stratocumulus clouds, *J. Atmos. Sci.*, *51*, 2434–2455, 1994a.

Cahalan, R. F., W. Rigdway, W. J. Wiscombe, S. Golmers, and Harshvardhan, Independent pixel and Monte Carlo estimates of stratocumulus albedo, *J. Atmos. Sci.*, *51*, 3776–3790, 1994b.

Cess, R. D., et al., Absorption of Solar radiation by clouds: Observations versus model, *Science, 267*, 496–499, 1995.

Coakley, J. A., Jr., and P. Chylek, The two-stream approximation in radiative transfer: Including the angle of the incident radiation, *J. Atmos. Sci., 32*, 409–418, 1975.

Davis, A., P. Gabriel, S. Lovejoy, D. Schertzer, and G. L. Austin, Discrete angle radiative transfer, 3, Numerical results and meteorological applications, *J. Geophys. Res., 95*, 11,729–11,742, 1990.

Davis, A., A. Marshak, and W. Wiscombe, Bi-multifractal analysis and multi-affine modeling of non stationary geophysical processes, Application to turbulence and clouds, *Fractals, 3*, 560–567, 1993.

Duroure, C., and B. Guillemet, Analyse des hétérogénéités spatiales des stratocumulus et cumulus, *Atmos. Res., 25*, 331–350, 1990.

Evans, K. F., and G. I. Stephens, A fast multidimensional radiative transfer model, in *IRS 92: Current Problems in Atmospheric Radiation*, edited by S. Kreevallik and O. Karner, pp. 473–476, A. Deepak, Hampton, Va., 1993.

Fouquart, Y., J. C. Buriez, M. Herman, and R. S. Kaendel, The influence of clouds on radiation: A climate modeling perspective, *Rev. Geophys., 28*, 145–166, 1990.

Frisch, U., *Turbulence*, 296 pp., Cambridge Univ. Press, New York, 1996.

Gabriel, P., S. Lovejoy, A. Davis, D. Schertzer, and G. L. Austin, Discrete angle radiative transfer, 2, Renormalization approach for homogeneous and fractal clouds, *J. Geophys. Res., 95*, 11,717–11,728, 1990.

Gierens, K. M., A fast six flux radiative transfer method for application in finite cloud models, *Rep. 2*, Inst. Phys. Atmos., Dtsch. Forsch. und Versuchsanst. für Luft- und Raumfahrt, Oberpfaffenhoffen, Germany, 1993.

Hentschel, H. G. E., and I. Procaccia, The infinite number of generalised dimension of fractals and strange attractors, *Physica D, 8*, 435–444, 1983.

Iaquinta, J., Development of a physically based bidirectional reflectance model of vegetation, *IEEE Trans. Geosci. Remote Sens.*, in press, 1996.

Joseph, J. H., and R. F. Cahalan, Nearest neighbor spacing of fair weather cumulus clouds, *J. Appl. Meteorol., 93*, 2405–2416, 1990.

Joseph, J. H., and V. Kagan, The reflection of solar radiation from bar cloud arrays, *J. Geophys. Res., 93*, 2405–2416, 1988.

Joseph, J. H., W. J. Wiscombe, and J. A. Weinman, The delta-Eddington approximation for radiative flux transfer, *J. Atmos. Sci., 29*, 793–805, 1976.

Lovejoy, S., Area-perimeter relation for rain and cloud area, *Science, 216*, 185–187, 1982.

Lovejoy, S., and D. Schertzer, Multifractal in geophysics, paper presented at Spring Meeting, AGU, Montreal, Canada, May 12, 1992.

Lovejoy, S., A. Davis, P. Gabriel, D. Schertzer, and G. L. Austin, Discrete angle radiative transfer, 1, Scaling and similarity, universality and diffusion, *J. Geophys. Res., 95*, 11,699–11,715, 1990.

Mandelbrot, B. B., *The Fractal Geometry of Nature*, 468 pp., W. H. Freeman, New York, 1983.

Marshak, A., A. Davis, W. Wiscombe, and R. Cahalan, Bounded cascade models as non-stationary multifractals, *Phys. Rev. E Stat. Phys. Plasmas Fluids Relat. Interdiscip. Top., 49*, 55–69, 1994.

Marshak, A., A. Davis, W. Wiscombe, and G. Titov, The verisimilitude of the independent pixel approximation used in cloud remote sensing, *Remote Sens. Environ., 52*, 71–78, 1995.

Meador, W. E., and W. R. Weaver, Two stream approximations to radiative transfer in planetary atmospheres: A unified description of existing methods and a new improvement, *J. Atmos. Sci., 37*, 630–643, 1980.

Mikhaylov, G. A., Asymptotic behavior of the average irradiance intensity for some models of stochastic media, *Izv. Russ. Acad. Sci. Atmos. Oceanic Phys.*, Engl. Transl., *18*(12), 993–997, 1982.

Monin, A., and A. M. Yaglom, *Statistical Fluid Mechanics*, vol. 1, 769 pp., MIT Press, Cambridge, Mass., 1975a.

Monin, A., and A. M. Yaglom, *Statistical Fluid Mechanics*, vol. 2, 974 pp., MIT Press, Cambridge, Mass., 1975b.

Parisi, G., and U. Frisch, A multifractal model of intermittency, in *Turbulence and Predictability in Geophysical Fluid Dynamics*, edited by M. Ghil, R. Benzi, and G. Parizi, pp. 84–88, North-Holland, New York, 1985.

Ramanathan, V., B. Subasilar, G. Zang, W. Connant, R. Cess, J. Kiehl, H. Grassl, and L. Shi, Warm pool heat budget and shortwave cloud forcing: A missing physics?, *Science, 267*, 499–503, 1995.

Schertzer, D., and S. Lovejoy, Physical modeling and analysis of rain clouds by anisotropic scaling multiplicative processes, *J. Geophys. Res., 92*, 9693–9714, 1987.

Schertzer, D., and S. Lovejoy (Eds.), Scaling non linear variability in geodynamics: Multiple singularities, observables, universality classes, in *Nonlinear Variability in Geophysics, Scaling and Fractals*, pp. 41–82, Kluwer Acad., Norwell, Mass., 1991.

Schmetz, J., On the parameterization of the radiative properties of broken clouds, *Tellus, Ser. A, 36*, 417–432, 1984.

Stephens, G. L., Radiation profiles in extended water cloud, I, Theory, *J. Atmos. Sci., 35*, 2111–2122, 1978a.

Stephens, G. L., Radiation profiles in extended water cloud, II, Parametrization schemes, *J. Atmos. Sci., 35*, 2123–2132, 1978b.

Stephens, G. L., and S. Tsay, On the cloud absorption anomaly, *Q. J. R. Meteorol. Soc., 116*, 671–704, 1990.

Tessier, Y., S. Lovejoy, and D. Schertzer, Universal multifractals: Theory and observations for rain and clouds, *J. Appl. Meteorol., 32*, 223–250, 1993.

Weinman, J. A., and P. N. Swarztrauber, Albedo of striated medium of isotropically scattering particles, *J. Atmos. Sci., 25*, 497–501, 1968.

Welch, R. M., and B. A. Wielicki, Stratocumulus cloud field reflected fluxes: The effect of cloud shape, *J. Atmos. Sci., 41*, 3085–3103, 1984.

Welch, R. M., and W. G. Zdunkowski, Backscattering approximations and their influence on Eddington-type solar flux calculations, *Contrib. Atmos. Phys., 55*, 28–42, 1982.

Wendling, P., Albedo and reflected radiance of horizontally inhomogeneous clouds, *J. Atmos. Sci., 34*, 642–650, 1977.

Zdunkowski, W. G., R. M. Welch, and G. Korb, An investigation of the structure of typical two-stream methods for the calculation of solar fluxes and heating rates in clouds, *Contrib. Atmos. Phys., 53*, 147–166, 1980.

R. Borde and H. Isaka, Laboratoire de Météorologie Physique, Université Blaise Pascal, 24, avenue des Landais, 63177 Aubière, France. (e-mail: borde@opgc.univ-bpclermont.fr)

(Received March 4, 1995; revised June 27, 1996;
accepted June 27, 1996.)